

2023

## Comparative Study of MOF's in Phosphate Adsorption

Eniya Karunamurthy  
*Wright State University*

Follow this and additional works at: [https://corescholar.libraries.wright.edu/etd\\_all](https://corescholar.libraries.wright.edu/etd_all)



Part of the [Engineering Science and Materials Commons](#)

---

### Repository Citation

Karunamurthy, Eniya, "Comparative Study of MOF's in Phosphate Adsorption" (2023). *Browse all Theses and Dissertations*. 2810.

[https://corescholar.libraries.wright.edu/etd\\_all/2810](https://corescholar.libraries.wright.edu/etd_all/2810)

This Thesis is brought to you for free and open access by the Theses and Dissertations at CORE Scholar. It has been accepted for inclusion in Browse all Theses and Dissertations by an authorized administrator of CORE Scholar. For more information, please contact [library-corescholar@wright.edu](mailto:library-corescholar@wright.edu).

# COMPARATIVE STUDY OF MOF'S IN PHOSPHATE ADSORPTION

A thesis submitted in partial fulfillment of the requirements for the degree of Master of Science in  
Materials Science and Engineering

By

ENIYA KARUAMURTHY

B.E., ANNA UNIVERSITY, INDIA, 2017

2023

WRIGHT STATE UNIVERSITY

WRIGHT STATE UNIVERSITY  
COLLEGE OF GRADUATE PROGRAMS AND HONOR STUDIES

04/24/2023

I HEREBY RECOMMEND THAT THE THESIS PREPARED UNDER MY SUPERVISION  
BY Eniya Karunamurthy ENTITLED Comparative Study of MOFs in Phosphate Adsorption  
BE ACCEPTED IN PARTIAL FULFILLMENT OF THE REQUIREMENTS FOR THE  
DEGREE OF Master of Science in Materials Science and Engineering.

---

Henry D. Young, Ph.D  
Thesis Director

---

Raghavan Srinivasan, Ph.D., P.E.  
Chair, Mechanical and Materials  
Engineering Department

Committee on Final Examination:

---

Henry D. Young, Ph.D

---

Malikarjuna N. Nadagouda, Ph.D

---

Hong Huang, Ph.D

---

Shu Schiller, Ph.D.  
Interim Dean  
College of Graduate Programs & Honor Studies

## ABSTRACT

Karunamurthy, Eniya. M.S.M.S.E., Department of Mechanical and Materials Engineering, Wright State University, 2023. Comparative Study of MOFs in Phosphate Adsorption.

High concentrations of phosphate are known to adversely affect the environment. Excess phosphate can lead to eutrophication that eventually fosters uncontrollable growth of aquatic plants and algae. This can result in depletion of oxygen content which adversely impacts underwater organism's survival rates. Metal organic frameworks (MOFs) consist of organic linkers in conjunction with metal ions or clusters arranged within a crystalline structure. They are highly porous and have larger surface area due to their ability to possess extensive void spaces while remaining bulky in nature. MOFs can absorb phosphate from aqueous solutions.

We have investigated the use of commercially available MOFs to extract phosphate. In this project, activated carbon was utilized as a control sample to compare the adsorption capacity of Metal-Organic Frameworks (MOFs), specifically evaluating Basolite C300, Basolite Z1200, Basolite A100, Basolite F300 and Basolite Z377. Three different pH solutions such as 5, 7, and 9 were used to study the influence of pH in adsorption. The scope of research encompasses both kinetics and Freundlich isotherm assessments. Scanning Electron Microscopy (SEM), Elemental Dispersive X-Ray Analysis (EDAX) and X-Ray Diffraction (XRD) techniques employed to study the MOFs in both pre- and post-adsorption analyses. It was found that some of the MOFs have better adsorption capacity when compared to other adsorbents.

**Keywords:** Metal organic frameworks, phosphate adsorption, Freundlich isotherm, capacity

## TABLE OF CONTENTS

1. INTRODUCTION.....	1
2. SCOPE OF THE THESIS.....	5
3. MATERIALS BACKGROUND.....	7
3.1. INTRODUCTION .....	7
3.2. ACTIVATED CARBON.....	7
3.3. METAL ORGANIC FRAMEWORKS.....	8
3.3.1. Basolite C300.....	11
3.3.2. Basolite Z1200.....	13
3.3.3. Basolite A100.....	14
3.3.4. Basolite F300.....	15
3.3.5. Basolite Z377.....	16
4. LITERATURE REVIEW.....	17
4.1. ACTIVATED CARBON IN PHOSPHATE ADSORPTION.....	17
4.2. MOFs in PHOSPHATE ADSORPTION.....	19
5. CHARACTERIZATION TECHNIQUES.....	24
5.1. INTRODUCTION.....	24
5.2. SPECTROPHOTOMETER.....	25
5.3. X-RAY DIFFRACTION.....	27
5.4. SCANNING ELECTRON MICROSCOPE.....	30
5.5. ELECTRON DISPERSIVE X-RAY ANALYSIS.....	33

6. EXPERIMENTAL.....	35
6.1. KINETICS EXPERIMENTS.....	35
6.1.1. Chemicals required.....	36
6.1.2. Equipment required.....	37
6.1.3. Others.....	37
6.1.4. Procedure.....	37
6.2. ISOTHERM EXPERIMENTS.....	39
6.2.1. Freundlich Isotherm.....	40
6.2.1.1. Procedure.....	42
7. RESULTS AND DISCUSSION.....	43
7.1. ADSORPTION KINETICS.....	43
7.1.1. Spectrometer Results and Adsorption Capacity.....	43
7.1.2. X-Ray Diffraction.....	47
7.1.3. SEM Images.....	50
7.1.4. EDS Results.....	52
7.1.5. TEM and STEM.....	55
7.2. ADSORPTION ISOTHERM.....	57
7.2.1. SPECTROMETER RESULTS AND ADSORBTION CAPACITY.....	57
7.2.2. FREUNDLICH ISOTHERM RESULTS.....	62
7.2.3. X-RAY DIFFRACTION.....	65
7.2.4.SEM.....	65
7.2.5. EDS.....	65

7.3. FACTORS AFFECTING ADSORPTION.....	67
7.4. MASS VS CONCENTRATION.....	68
8. CONCLUSION AND FUTURE WORK.....	70
9. REFERENCES.....	71

## LIST OF FIGURES

Figure 1, Algae Boom, Lake Erie.....	3
Figure.2, Activated Carbon Structure.....	8
Figure 3, Synthesis methods of MOF.....	9
Figure 4, Basolite C300.....	12
Figure 5, Basolite Z1200.....	13
Figure 6, Basolite A100.....	14
Figure 7, Basolite F 300.....	15
Figure 8, Basolite Z377.....	16
Figure 9, Changes in the pH with time during CDI adsorption at various applied voltages.....	18
Figure 10, Comparison of MOFs with Y-zeolite in adsorption.....	21
Figure 11, Adsorption-desorption N <sub>2</sub> isotherms for Basolite F300. N <sub>2</sub> Vs Relative pressure.....	22
Figure 12, Spectrophotometer principle.....	26
Figure 13, HACH D1900 portable spectrophotometer.....	27
Figure 14, X-Ray Diffraction Principle.....	29
Figure 15, Scanning Electron microscope.....	32
Figure 16, Principle of EDS.....	33
Figure 17, General Procedure of Adsorption Experiments.....	38
Figure 18, Concentration Vs Time, Kinetics graph of pH 5.....	44

Figure 19, Concentration Vs Time, Kinetics graph of pH 7.....	45
Figure 20, Concentration Vs Time, Kinetics graph of pH 9.....	47
Figure 21, XRD images of the adsorbents before and after adsorption.....	49
Figure 22, SEM images of the adsorbents before and after adsorption.....	51
Figure 23, EDAX graph of the adsorbents before and after adsorption.....	55
Figure 24, TEM images of the adsorbents after adsorption.....	57
Figure 25, STEM image - Basolite Z1200.....	57
Figure 26, Concentration Vs Time graph of pH 5 after 2 weeks.....	59
Figure 27, Concentration Vs Time graph of pH 7 after 2 weeks.....	60
Figure 28, Concentration Vs Time graph of pH 7 after 2 weeks.....	61
Figure 29, Freundlich Isotherm plot, log final conc vs log capacity.....	64
Figure 30, EDAX graph of the adsorbents after adsorption.....	67
Figure 31, Mass vs Concentration and Mass vs Capacity graph.....	69

## LIST OF TABLES

Table.1, Spectrophotometer readings of pH 5 and the calculated capacity.....	43
Table.2, Spectrophotometer readings of pH 7 and the calculated capacity.....	45
Table.3, Spectrophotometer readings of pH 9 and the calculated capacity.....	46
Table.4, Spectrophotometer readings of pH 5 after 14 days and the calculated capacity..	58
Table.5, Spectrophotometer readings of pH 7 after 14 days and the calculated capacity..	59
Table.6, Spectrophotometer readings of pH 9 after 14 days and the calculated capacity..	61
Table 7, Freundlich Isotherm Calculations for pH 5.....	62
Table 8, Freundlich Isotherm Calculations for pH 7.....	64
Table 9, Freundlich Isotherm Calculations for pH 9.....	65
Table.10, Capacity vs Surface Area.....	67
Table.11, Mass vs Concentration and Capacity.....	68

## ACKNOWLEDGEMENT

I would like to express my deepest gratitude to my advisor, Dr. Daniel Young, for his unwavering support and guidance throughout my research journey. His expert advice, feedback, and constant encouragement were invaluable in shaping my academic journey. His enthusiasm and passion towards Materials Science is an inspiration for me to learn more.

This endeavor would not have been possible without Dr. Mallikarjuna Nadagouda, who generously provided knowledge and expertise. Additionally, this would have been difficult without the generous support from Pegasus Technical Services Inc, who financed my research.

I would like to extend my sincere thanks to Dr. Raghu Srinivasan, for his valuable suggestions and guidance.

I would also like to extend my heartfelt thanks to my parents Mrs. Kalaichelvi, and Mr. Karunamurthy for their constant love, and support. Also, my sister Mrs. Edhaya for her encouragement and motivation.

I would like to acknowledge my close friends who have been a source of strength and motivation throughout this entire journey. Their presence in my life has made this journey more enjoyable and fulfilling.

Lastly, I would like to thank myself for the perseverance, hard work, and dedication that I have put into this research project. This process has challenged me in countless ways and has helped me grow both personally and professionally.

# 1. INTRODUCTION

Phosphorus is a typical part of sewage and industrial effluent organic wastes, manure, and agricultural fertilizers. Although it is a necessary component for plant life, excessive amounts can hasten the rivers and lakes becoming eutrophic. Soil erosion is a substantial contributor to phosphorus in streams. Floods can result in bank erosion, which can release a lot of phosphorous from surrounding land and riverbanks into a stream, lake, or other body of water.

Phosphorus naturally exists in mineral deposits and in rocks. Chemical substances containing phosphorus are known as phosphates. As the mineralized phosphate compounds disintegrate, the phosphorus slowly leaks out of the rocks as soluble phosphate ions during the natural weathering process. There are three types of phosphates: orthophosphate, metaphosphate (also known as polyphosphate), and phosphate that is attached to an organic substance. These phosphates can be discovered in soil, rocks, and aquatic systems as free ions or as compounds. They can also be discovered in the remains of dead and live animals and plants. [1]

In lake ecosystems, phosphorus tends to be the growth-limiting nutrient since it is essential for the Krebs Cycle, the production of ATP (adenosine triphosphate), and DNA. Phosphorus is also one of the essential nutrients for the growth of plants and animals. Well-oxygenated lake waters frequently lack phosphorus, and this is significant since the lack of phosphorus restricts the growth of freshwater systems. In contrast to nitrogen, phosphate is kept in the soil by a sophisticated biological uptake, absorption, and mineralization system.

Unless they are present in extremely high concentrations, phosphorus is neither hazardous to humans nor animals. Extremely high phosphate levels may cause digestive issues. Animals and plants utilize the soluble or bio-available orthophosphate after that. Phosphate is incorporated

into the biological system, although ATP, DNA, and RNA are the main components. Adenosine triphosphate, or ATP, has a significant role in the Krebs Cycle, and is also crucial for storing and utilizing energy. The genetic foundation of life on this planet is made up of RNA and DNA. As a result, one of the major factors affecting photosynthesis is the availability of phosphorus. Even though phosphorus has been used, the excess amount of phosphorus is harmful to the environment. Phosphates also infiltrate streams from artificial sources such as organic wastes in sewage and industrial effluent, manure, and agricultural fertilizers. Our contribution per person is about 3.5 pounds.

Upon research, it has been determined that the utilization of phosphorus-rich fertilizer may give rise to unfavorable consequences for bodies of water. The existence of this chemical leads to a boost in algal proliferation which causes oxygen levels within aquatic ecosystems to plummet resulting in an untimely demise amongst several species of fish and other components affected by these environments. Local water resources are put at risk when these deposits become exposed, leading to contamination. As it contains phosphorus, when immersed in water the potential for algal blooms is high. These vibrant algae formations are known to deplete oxygen levels within aquatic environments leading to fatalities amongst various marine species including fish and other organisms residing underwater. The effects on both areas should not be minimized and overlooked.



Figure 1, Algae Bloom, Lake Erie, 2011 [2]

This photo depicts the worst bacterial bloom Erie Lake has seen in many years. It is the green slime that is seen. In the 1950s and 1960s, the shallow western basin of the lake, such blooms were common. Huge algae blooms continued to grow year after year thanks to the phosphorus that farms, sewage, and industry added to the water. Heavy winter and spring snowfall created snowmelt flow, which was then followed by a torrent of rain in April. When water poured from fields, yards, and paved surfaces, rain and melting snow transported a variety of pollutants into streams and rivers, including phosphorus and nitrogen from fertilizers. Increased rain and runoff produced additional phosphorus, a substance that fed the lake's algae. The bloom is not beneficial for marine life, despite not being immediately poisonous to fish. The dead algae are broken down by a bacterium. Due to the oxygen depletion caused by the decay process, the collapse of a large bloom can create "dead zones," low oxygen areas where fish cannot survive. The algae may kill pets if consumed, but it may also give people flu-like symptoms.

To varied degrees of success, phosphate levels are reduced once they have entered the water system using a variety of techniques. Adding chemicals to sewage, like ferric sulphate, is one typical approach for reducing phosphate levels before any processing begins. However, it is

projected that the price of these chemicals will increase in the future, and they can also cause an increase in iron levels, which may require its own treatment, making it less practical as a long-term solution.

Sand filtration is an alternative. This method still requires the addition of chemicals to wastewater when it enters a sewage treatment facility, but the phosphates are easily removed once the water has been passed through vertical sand filters. Some water treatment facilities employ certain bacterial species that may extract phosphates from the sludge by absorbing up to 20% of their own mass. Several of these techniques only work well in enclosed spaces like water treatment plants; they do not deal with the problem of agricultural run-off or other sources of excess phosphates. They also come with their own set of financial and ecological problems. [2]

## 2. SCOPE OF THE THESIS

Much research has been conducted all around the world to find ways to remove excess phosphorus from water bodies to protect the environment. This project is a collaboration with the Environment Protection Agency (EPA), Cincinnati, Ohio where they conduct various research to protect humans and the environment. Among that research, effective removal of phosphate from the water around Dayton and Cincinnati areas is one of them. They have reported results using various materials which work effectively in phosphate removal from the list of around hundred materials.

Excess amounts of phosphorus are toxic to development and reproduction. In terms of phosphate in drinking water, there are several provisional health-based recommendations. With present treatment techniques, it is challenging to reduce phosphate levels in the environment to below the provisional standards. To reduce the harmful effects on both human health and the environment, treatment strategies for their removal are needed. Many previous studies have concentrated on chemical breakdown methods that require severe temperature or pressure requirements. These methods do, however, have certain drawbacks due to their high energy requirements and interference from other substances in wastewater. To specifically absorb and degrade phosphate into non-toxic chemicals, additional research into highly effective technology is necessary.

MOFs have countless benefits that set them apart from the top adsorbent options. MOFs with organic linkers and metallic nodes would be highly tunable in comparison to other adsorbents. Moreover, MOFs have highly variable pore diameters. MOFs have previously been used as photocatalysts for the treatment of wastewater as well as organic chemistry. MOFs will therefore

be used to photo-mineralize phosphates under UV and visible light. One major drawback when it comes to MOFs is that MOFs are expensive. In future, if the MOFs can be made less expensive, then they can be widely used in many more applications. The MOFs used for this research are Basolite C300, a copper-based MOF; Basolite Z1200, a zinc-based MOF; Basolite A100, an aluminum-based MOF; Basolite F 300, an iron-based MOF; Basolite Z 377, another zinc-based MOF. Activated Carbon is used as a control sample. The adsorbents were evaluated with three different pHs such as pH 5, pH 7, and pH 9 to evaluate the characteristics of adsorbents at different pHs. All the MOFs were bought from Sigma-Aldrich and were used in as in condition. By using powder X-ray diffraction, scanning electron microscopy (SEM), and transmission electron microscopy (TEM), MOFs were characterized, and their capacity to absorb Phosphate was calculated.

### 3. MATERIALS BACKGROUND

#### 3.1. INTRODUCTION

Phosphate has been removed from water bodies using activated carbon, limestone, alumina, iron oxide, silver nanoparticles, zeolites, clay, iron oxides, and lanthanum-based materials. calcium carbonate etc., Even though there are many materials available, there are some limitations with the existing materials. The adsorbents reach saturation point and more adsorbents are needed for higher concentration phosphate holding water bodies. Also, some adsorbents are not recyclable and regeneratable. Here the activated carbon has been used as a control sample to compare the MOFs to show their ability.[17]

#### 3.2. ACTIVATED CARBON

Granular activated carbons are a type of adsorbent with many different uses. They can be used to selectively absorb a wide range of organic and certain inorganic compounds. From the charred interiors of whiskey barrels to the ancient Egyptian use of powdered carbons for medicine, carbon has already been generated and used as adsorbent since the dawn of time. The first common application of granular activated carbon was in military gas masks during World War I and later in commercial solvent recovery systems. Following World War, I, the de-colorization of sugar and the purification of antibiotics were the activated carbons' first well-known applications. Hundreds of applications are currently in use; thousands of applications would be in use if distinct purposes that fall under the category of environmental management were counted individually.

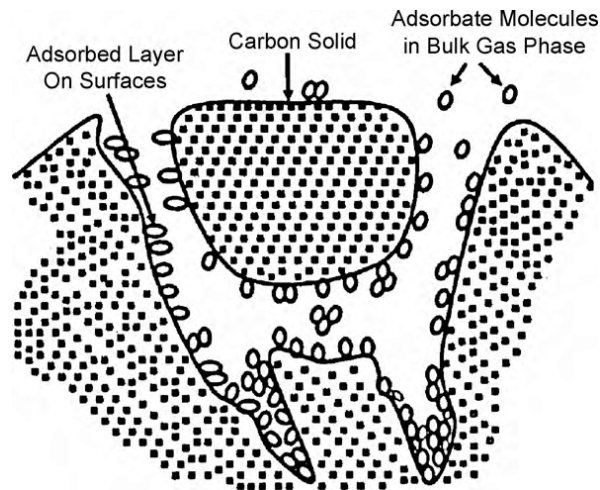


Figure.2, Activated Carbon Structure [9]

During production of activated carbon, both chemical and thermal procedures removed the majority of the unstable non-carbon components and a come of the natural carbon composition, leaving a material with a huge surface area, when magnified by electron microscopy appears as a structure that resembles a sponge.

Since the carbon surface is often non-polar, it has no electrical charge. Because they are non-polar, activated carbon surfaces have a strong attraction for non-polar adsorbates like most organics. In this way, activated carbon is different from neutral desiccating sorbent materials like silica gel and processed aluminum oxide. By capillary condensation, granular activated carbon will show a slight dislike of water, but not the desiccant-like interfacial attraction to water. [3]

### 3.3. METAL ORGANIC FRAMEWORKS

Metal-organic frameworks (MOFs) are an intriguing family of materials that have received a great deal of interest lately. These substances are made of a highly porous and crystalline network of metal ions or clusters connected by organic ligands. MOFs are appealing for a variety

of uses, such as gas storage, separation, catalysis, and sensing. The resultant structure resembles a molecular sponge with a large surface area.

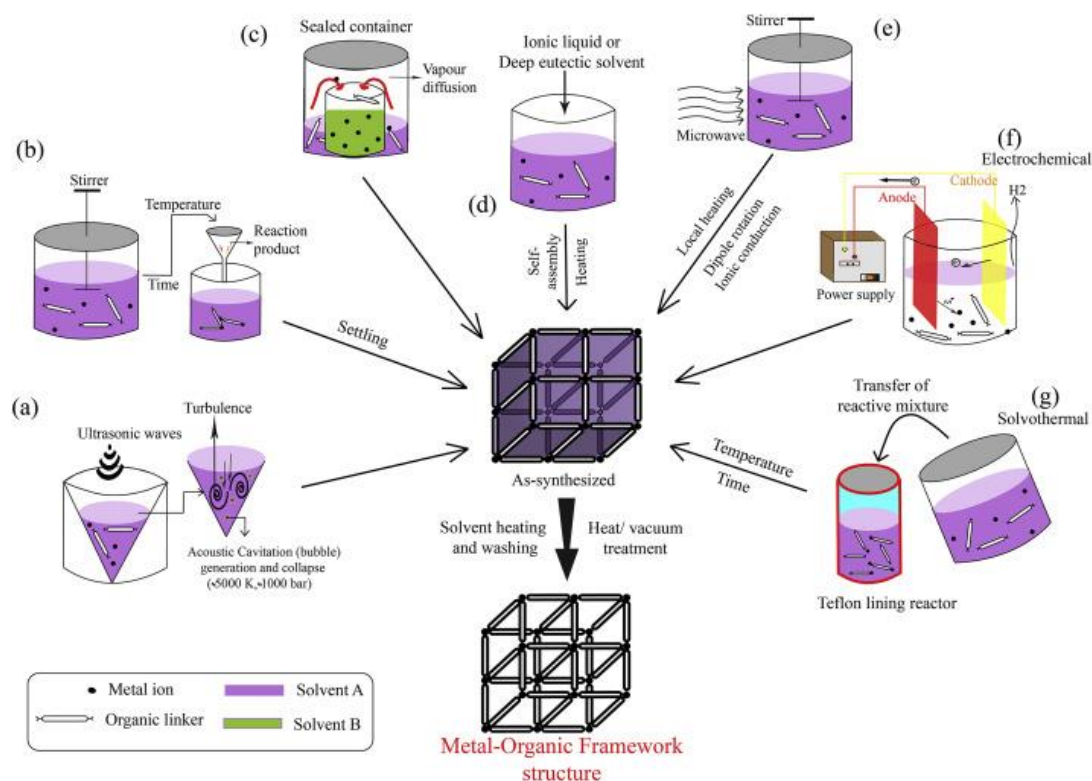


Figure 3, Synthesis methods of MOF [16]

Zinc, copper, chromium, aluminum, magnesium, lanthanide, and other metal ions with particularly intriguing characteristics are often utilized in the production of MOFs. Organic ligands need functional groups with nitrogen or oxygen, such as amide or nitrile groups, to have a lone electron pair to coordinate a metallic center (e.g., carboxylic groups). Also, each metal center must work with two or more of them. According to their electric charge, organic ligands can be classified as neutral, positive, or negative.

The new synthesis techniques use low-temperature reactions, including some that occur at room temperature, which are continuously stirred in an open system. The duration of these syntheses

might range from a few seconds to several hours. Microwave radiation or ultrasound are often employed to shorten the processing time. Other techniques for producing MOFs include electrochemical and mechanical chemical synthesis. The solvent molecules bound at open coordination sites in MOFs need to be released for these materials to have the necessary adsorption characteristics. In this stage, chemical and thermal activation are employed (along with other solvents). One area of active research is efficient benzene vapor adsorbents. [8]

Scientists' study of crystalline aluminosilicate minerals known as zeolites for gas separation and catalysis by scientists led to the discovery of MOFs in the late 1990s. They discovered that the organic part used to make zeolites could be swapped out for different organic ligands, resulting in the development of a brand-new category of materials called MOFs.

The enormously large surface area of MOFs is one of its most striking characteristics. It is possible to precisely regulate the properties of the material by adjusting the size and form of the pores inside the framework. In comparison to conventional porous materials like activated carbon or zeolites, MOFs have orders of magnitude greater surface areas per gram, ranging from hundreds to thousands of square meters.

MOFs are more suitable materials for gas storage and separation due to their enormous surface area. To advance renewable energy technologies like fuel cells, researchers have shown that MOFs may be used to store and release significant amounts of hydrogen. Moreover, MOFs have been used to separate various gases, including carbon dioxide and methane, which is essential for carbon capture and storage.[19]

The use of MOFs in catalysis is a promising new application. Since reactants and products can diffuse easily through MOFs' porous structure, catalytic processes on these materials have an

enormous potential for efficiency. Researchers have proven the versatility of MOFs as catalysts, demonstrating their ability to produce hydrogen from water and transform biomass into valuable compounds.

MOFs could also be used for drug delivery and sensing. MOFs are beneficial for drug delivery because the holes within the framework can be exploited to trap and release molecules. MOFs can be used as sensors for a variety of analytes since modifications to their structure or composition can also affect their electrical or optical characteristics. [20]

Although MOFs have a wide range of uses, there are still some issues that must be resolved before their widespread adoption in industry. Since MOFs might be susceptible to moisture and other environmental conditions, stability in various environments is a significant concern. More stable MOFs that can survive a wider range of environments are currently being developed by researchers. In summary, MOFs are an intriguing class of materials that have the potential to completely transform a wide range of sectors. MOFs have a high surface area, fine control over pore size and form, and a variety of applications, making them a prospective area for future research and development. We are likely to see these materials taking on a bigger role in a variety of disciplines as we continue to learn more about them and overcome their obstacles.[16]

### **3.3.1. Basolite C300**

Basolite also Copper benzene-1,3,5-tricarboxylate, Cu-BTC MOF or HKUST-1. The Empirical Formula is  $C_{18}H_6Cu_3O_{12}$ . The Molecular mass is 604.87 and the particle size distribution is 15.95  $\mu\text{m}$  with a surface area of 1510-2110  $\text{m}^2/\text{g}$  and a bulk density of 0.35  $\text{g}/\text{cm}^3$ .

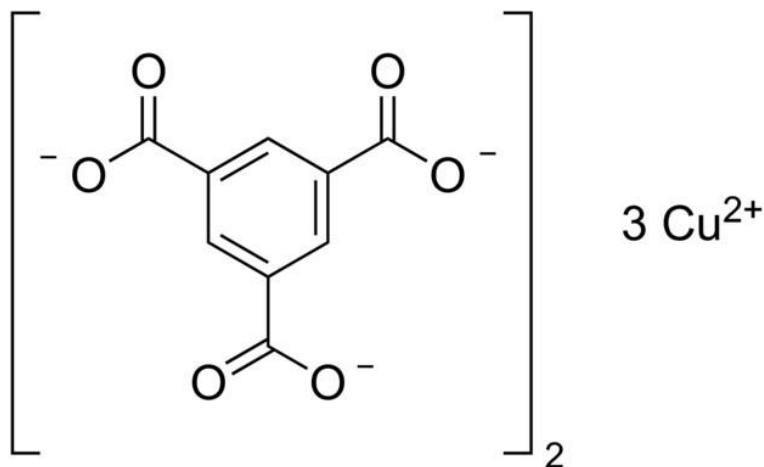


Figure 4, Basolite C300 source: [HKUST-1, Cu-BTC Basolite C300 produced by BASF HKUST-1 \(sigmaaldrich.com\)](#)

Basolite C 300 is a metal organic framework (MOF) which is a hybrid porous solid that has crystallized from inorganic subunits joined by organic linkers like carboxylates or phosphonates. It is a commercially available adsorbent with the HKUST-1 structure. Other names for HKUST-1 include Cu-BTC, MOF-199, and Basolite(TM) C300. A copper-based ultra microporous metal framework, HKUST-1 is a blue cubic crystal (MOF). Solvothermal preparation is used to prepare it. Almost 2200 m<sup>2</sup>/g of surface area is possible. CO<sub>2</sub>, CO, and adsorption of dibenzothiophene can all be absorbed using Basolite C 300. It is also used for catalysis, separations, and gas storage. One benefit of employing C300 for adsorption is that it is simple to replenish the C300 adsorbent by rinsing with lightweight alcohols. The new C300's adsorption capability can be perfectly recovered upon regeneration with methanol. Whereas the sorbent that has been refreshed with methanol at 305 K preserves all its crystallinity, the used C300 loses crystallinity due to adsorption. It is possible to complete three regeneration cycles without any obvious adsorption capacity reduction. [4]

### 3.3.2. Basolite Z1200

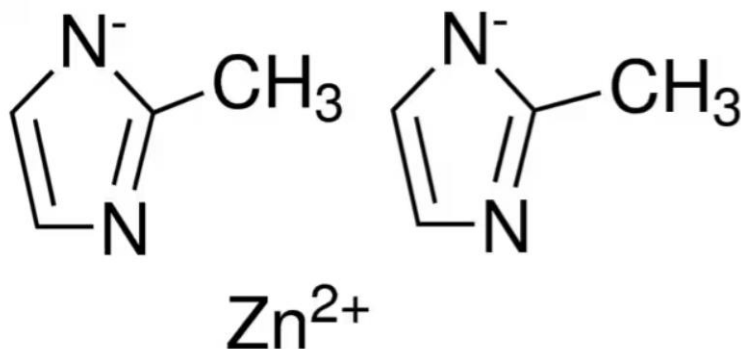


Figure 5, Basolite Z1200 source: [Basolite Z1200 produced by BASF 59061-53-9 \(sigmaaldrich.com\)](https://www.sigmaaldrich.com)

Basolite also 2-Methylimidazole zinc salt, ZIF-8. The simple Formula is C<sub>8</sub>H<sub>10</sub>N<sub>4</sub>Zn. The Molecular mass is 227.58. The particle size and surface area are 4.9 μm and 1310-1810 m<sup>2</sup>/g with a bulk density 0.36 g/cm<sup>3</sup>.

The zeolitic imidazolate framework (ZIF) in Basolite Z1200 is made up of metal ions and imidazolate anions. ZIF has a structure that is comparable to silica-zeolites. ZIFs exhibit excellent thermal stability.

The creation of matrix membranes for gas separation procedures like hydrogen separation and nitrogen recovery can be conducted using Basolite Z1200 (ZIF-8) based MOFs. Moreover, they are used as fillers when creating PDMS-based membranes for solvent-resistant nanofiltration (SRNF). For the absorption and detection of pesticides, they are used commercially as porous materials. Moreover, it is employed for gas adsorption, sensors, and separations (alkanes and paraffin isomers) (hydrogen gas).

The thermal, hydrothermal, and chemical stabilities of Basolite Z1200 were often better. Basolite (ZIF 8) is well known for its uses in separation, gas storage, chemical sensors, and catalysis. ZIF 8 can be used to create filters to remove pesticide from a given sample. Basolite Z1200 reactivation properties make it more affordable and suitable for long-term treatment systems. [5]

### 3.3.3. Basolite A100

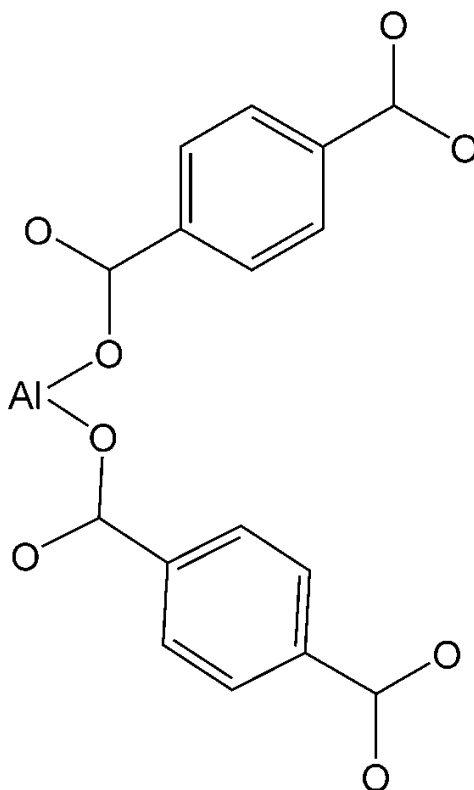


Figure 6, Basolite A100 [6]

Basolite A100 also Aluminum terephthalate, MIL-53(Al). The Formula is  $C_8H_5AlO_5$ . The Molecular mass is 208.10. The particle size distribution and surface area are 31.55  $\mu m$  1110-1510  $m^2/g$  respectively with a bulk density of 0.39  $g/cm^3$ .

MIL-53 is another name for Basolite A100 (Al). A microporous metal-organic framework (MOF) with micropores up to nine hundred pm in diameter, Basolite A100 is made up of three-dimensional networks. Due to the presence of octahedral  $\text{AlO}_4(\text{OH})_2$  units linked by 1,4-benzenedicarboxylate ligands, it shows properties that are exactly like those of MIL-53(Al). It allows the development of a structure with a high specific surface area of  $1084 \text{ m}^2\text{g}^{-1}$  and a pore volume of  $0.51 \text{ cm}^3\text{g}^{-1}$ . C8-alkylaromatic compound separation was conducted using Basolite A100.

The primary application of Basolite A100 is in the binary gas separation of  $\text{CO}_2/\text{CH}_4$  and  $\text{CO}_2/\text{N}_2$ . Additionally, it can be applied to the supercritical adsorption of  $\text{CO}_2$  and the gas adsorption of hydrogen gas.

#### 3.3.4. Basolite F300

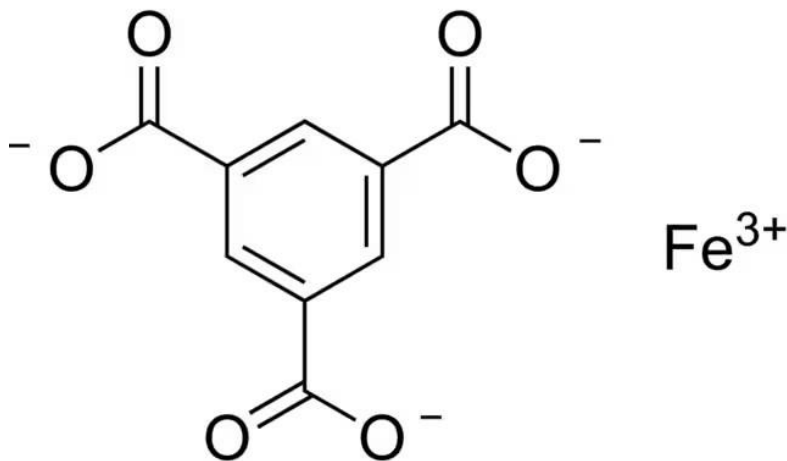


Figure 7, Basolite F 300 source: [Basolite F300 produced by BASF 1195763-37-1 \(sigmaaldrich.com\)](https://www.sigmaaldrich.com)

Basolite F300 also Fe-BTC, Iron 1,3,5-benzenetricarboxylate has the Formula of  $\text{C}_9\text{H}_3\text{FeO}_6$  and has a molecular mass of 262.96. The surface area and the bulk density are  $1300\text{-}1600 \text{ m}^2/\text{g}$  and  $0.16\text{-}0.35 \text{ g/cm}^3$ .

In Lewis acid processes like the acetalization of aldehydes and aldol condensation, Basolite F300 (Fe-BTC), a porous metal organic framework (MOF), is used as a highly effective catalyst. It is composed of oxo centered trimmers of an iron(III) octahedron joined by trimesate anions, giving it a hybrid super tetrahedral structure.

Fe-BTC based MOF can be used in environmentally friendly processes like energy storage using lithium-ion batteries. It can be applied to the supercritical CO<sub>2</sub> adsorption process as well.

### 3.3.5. Basolite Z377

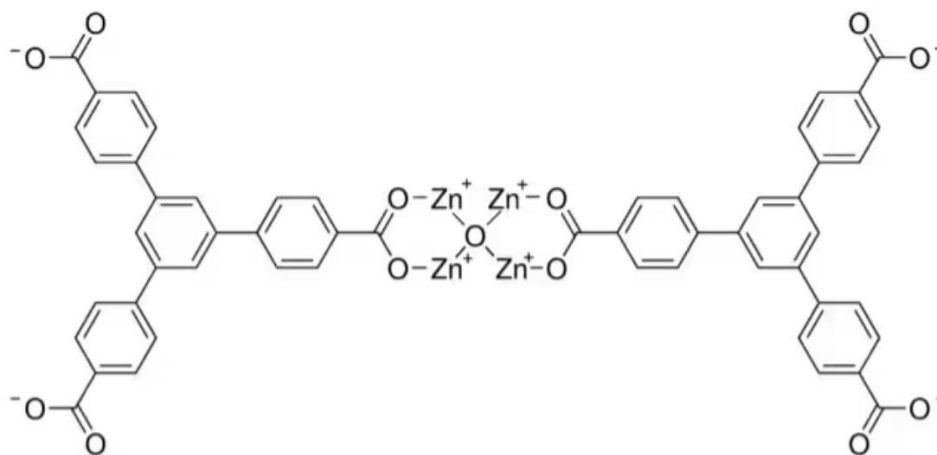


Figure 8, Basolite Z377 source: [Basolite Z377 MOF 177 676593-65-0 \(sigmaaldrich.com\)](https://www.sigmaaldrich.com)

Basolite Z377 also MOF 177 has the empirical formula of C<sub>54</sub>H<sub>30</sub>O<sub>13</sub>Zn<sub>4</sub> and a molecular weight of 1148.37. It includes Carbon 105 g/200g, Zinc (Zn) 44 g/200g ±10%. It has a surface area of 5010-5210 m<sup>2</sup>/g. Basolite Z377 is used for gas and pollutant adsorption and in adsorbing methane and hydrogen absorption. This MOF is comparatively expensive so there are few applications. Thermally decomposition temperature occurs above 400°C.

## 4. LITERATURE REVIEW

### 4.1. ACTIVATED CARBON IN PHOSPHATE ADSORPTION

Fang-Fang Chen et al., studied the activated carbon electrodes in phosphate adsorption. The largest adsorption capacity was determined to be 8.53 mg/g. Following a specific time of adsorption, the electrodes present a certain level of saturation and are ready to be regenerated through potential reversal or short-circuiting mechanisms. The Capacitive Deionization process is connected closely with the physical as well as chemical traits intrinsic in electrode materials such as their pore size distribution, hydrophilicity, electrical conductivity and specific surface area properties that reveal varying levels of adsorption capabilities.

Researchers have been exploring various carbon-based materials with elevated specific surface areas to be highly proficient absorptive agents. Some of substances being studied were carbon aerogels, graphene sheets, carbon fibers, carbon nanotubes and activated charcoal. Activated carbon is a universally used porous electrode component in Capacitive Deionization (CDI) for multifarious reasons. The material boasts an elevated surface area, substantial porosity, and remarkable adsorption ability. Furthermore, in addition to these enticing features, activated carbon guarantees a low-cost differential, making it an economic choice. The study delved into the kinetics and thermodynamics of electro sorption in phosphate solutions at various voltages, temperatures, and concentrations to uncover how these factors affect phosphate adsorption by Capacitive deionization (CDI). Finding the Phosphate adsorption mechanism on CDI electrodes involved precise thermodynamic calculations. No applied voltage existed any electrostatic field between the two electrodes resulting in Phosphate in solution removal by mere absorption onto

activated carbon. The results showed a mere 6% removal efficiency coupled with only 0.08mg/g adsorption capacity eliminating activated carbon as a significant contributor to efficient phosphate removal from solution.

It has been determined that the ability for adsorption declines proportionally as initial pH values increase. As the initial pH range was between 6 to 10, the capacity for CDI, to adsorb Phosphate, witnessed a gradual decline from an amount of 3.8 mg/g down to 3.0 mg/g. An estimation could be made for the adsorption constant by examining the slope between the amount of phosphorus adsorbed and time elapsed; this calculation suggests that an experimental model known as the Freundlich isotherm more accurately described such data than did its counterpart, known as Langmuir isotherm model. It is believed that multilayer adsorption took place regarding electrified carbon electrode-based phosphorus absorption; notably, maximum available capacity amounted to approximately 8.53 mg/g under standard temperature conditions (298 K). Improvement in terms of additional adhesive areas emerged during said process, suggested in part through findings indicating that Freundlich Constant  $1/n$  was less than one: indicative of complimentary new sites having formed.

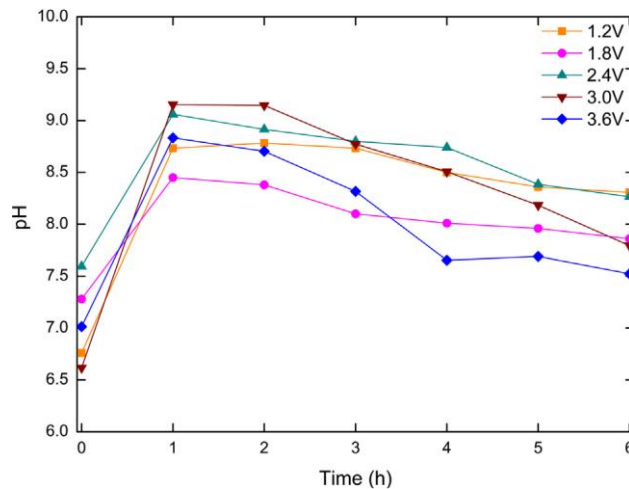


Figure 9, Changes in the pH with time during CDI adsorption at various applied voltages. [25]

Interestingly, they have observed that not every pore within activated carbon electrodes has the capacity to adsorb ions, and the level of concentration can significantly impact the effective inner surface area. The mechanism behind phosphate adsorption through Capacitive Deionization (CDI) was assessed using kinetics, thermodynamics, and equilibrium GCS models. It was found that as voltage increased, so did both adsorption capacity and removal efficiency. Following five rounds of adsorption-desorption experiments, an impressive 91% of initial adsorption capacity remained at a rate of 1.173mg/g. Furthermore, desorption hit a rate of 99.2% on its fifth round - indicating the homemade activated carbon electrode had strong regeneration ability post-phosphate-adsorption while also making CDI a feasible option for phosphate removal/recovery from aqueous solutions.[25]

#### 4.2. MOFs in PHOSPHATE ADSORPTION

Metal-Organic Frameworks, often abbreviated as MOFs, are fascinating compounds composed of metal ions or clusters working in tandem with rigid organic molecules. Hydrothermal and solvo-thermal techniques are the primary methods used to synthesize MOFs wherein crystals grow gradually from a heated solution. These remarkable frameworks rely heavily on the process of adsorption for removing harmful entities, and their overall structure and properties are highly dependent on the choice of metal-ion and linker used. The solvent plays a crucial role too, being the main molecule utilized for templating purposes. Adsorption proves to be a superior technique when it comes to eliminating toxic waste due to several reasons such as cost-effectiveness, ease of operation, design simplicity, broad spectrum applications along with minimal or non-existent generation of toxic by-products. Simply, it is defined as molecular species accumulation at the surface rather than getting absorbed internally. Based on various porous adsorbent materials like

activated carbons or mesoporous substrates that exist one standout is Metal-Organic Frameworks which wins over other candidates primarily zeolites and activated carbon because they offer unique advantages concerning performance characteristics.

Activated Carbon, though impressive when implemented, does come up short most prominently when it comes to tackling soluble organics by not uniformly removing all potential hazards present within an environment affected by pollutants. In contrast, MOFs do not have similar shortcomings mentioned earlier regarding its usage list owing to its structure bridging between organic ligands remaining intact end-to-end bindings during synthesis therefore remains uncontaminated restricting any deactivating effect seen in Zeolites-based adsorption systems.

In an article by P. Sagar et al., Y-Type Zeolites adsorption abilities scale unfavorably with MOFs since it is seen that the use of Metal Organic Frameworks such as Basolite C300, A100 and F300 show even higher DBT adsorption capacity compared to Y-type variations scrutinized in previous studies. Additionally, MOFs like C300 and A100 manage to retain more significant potential towards adsorbing hazardous materials than F300.

The objective of the experimentation was to record nitrogen adsorption-desorption isotherms for the three MOF systems (C300, A100, and F300) to delineate their textural properties and identify any variances in performance among them. An analysis of parameters, such as the specific BET area, pore size, and pore volume values revealed notable differences between C300 and F300 with regards to BET area value. Specifically, C300 displayed a superior BET area compared with its counterparts and subsequently demonstrated a substantial decrease in this parameter from F300 onwards.

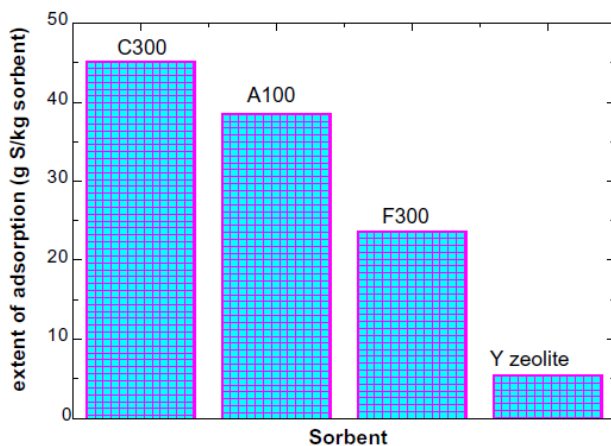


Figure 10, Comparison of MOFs with Y-zeolite in adsorption [26]

Adsorption has emerged as a crucial process in combatting dangerous substances, specifically within liquids and gases. MOFs possess exceptional adsorptive abilities towards various toxic ingredients based on their high surface area coverage attributable to a range of pore geometries which make them an ideal sorbent with enhanced adaptability due to configurable porosity levels upon functionalization. Overall, this makes them superior over other porous substances in terms of performance when it comes to the elimination of hazardous particles which continue to threaten human health and wellbeing. [26]

One of the main reasons for phosphate pollution is a broad spectrum of coloring agents and dyes, mixing with water bodies encompassing both industrial and household usage, have been categorized as residual hazardous materials by the US Environmental Protection Agency (EPA) as well as the European Union. Current wastewater treatments intended at curbing dyes come with costly and time-consuming implications yet remain less-than-adequate in meeting established regulatory standards for water quality. Fortunately, Fe-BTC MOFs or Basolite F300 present outstanding prospective material options availing valuable functionalities such as

selective adsorption processes, drug transport facilitation, catalysis exploitability along with sensing applications, among others.

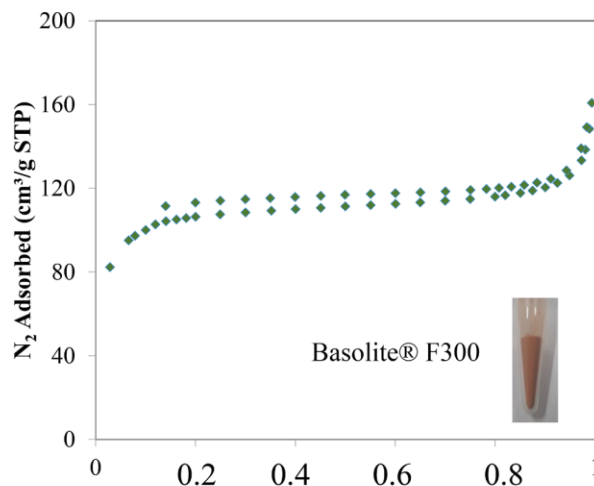


Figure 11, Adsorption-desorption N<sub>2</sub> isotherms for Basolite F300. N<sub>2</sub> Vs Relative pressure [27]

A research investigation by Conde-Gonzalez et al., was undertaken to examine the influence of the initial pH level on the adsorption potential of the created substance at standard temperature. The assessment was conducted over a spectrum of pH values that spanned from 2 to 9 and entailed deploying an initial dye concentration set at 200  $\mu\text{g}\cdot\text{L}^{-1}$ . The proportion of dye molecules adsorbed decreased notably to less than ten percent when pH values were above six. To analyze experimental data on dye adsorption isotherms, researchers employed two models: the Langmuir and Freundlich isotherm models. They then used nonlinear regression analysis to determine the optimal parameters for adsorption. Crucially, all the dyes molecules contain aromatic rings that may contribute to their overall performance in terms of undergoing successful adsorption processes. Regarding phosphate ions, increasing its concentration to 300  $\text{mg}\cdot\text{L}^{-1}$  resulted in a 25% decrease in adsorption rates for FL and Cl-FL dye molecules.

Numerous parameters were investigated, including sorbent quantity and adsorption equilibrium duration. As a result, the MOFs exhibited an adsorption efficiency exceeding 90% for each instance. Interestingly, wastewater only demonstrated abysmal results with less than 65% efficiency noted. Upon conducting adsorption-desorption tests on aqueous solvents using Dispersive Solid-Phase Extraction methodology, optimal results were obtained as hypothesized.[27]

## 5. CHARACTERIZATION TECHNIQUES

### 5.1. INTRODUCTION

To study materials characterization, one must observe and analyze characteristics at various levels, including atomic, molecular, and macroscopic levels. This facet is an integral aspect of engineering and science that enables us to comprehend material structure and composition in addition to their properties. The recognition obtained allows for enhancement of quality leading towards advanced functionality which fosters innovation through fabricating better mineral compounds.

The classification of characterization techniques can be split into two overarching types: functional and structural. Functional methods are utilized to comprehend the properties, qualities, or behavior patterns of a material such as its mechanical, thermal, or electrical attributes. On the other hand, Structural techniques concentrate on examining the atomic and molecular composition of materials, much like spectroscopy, and employ X-ray diffraction and electron microscopy for the same purpose.

Material characterization has a pivotal function in numerous fields like healthcare, energy, electronics, aerospace, and manufacturing. Understanding the mechanical properties of materials like metals or ceramics is crucial in maintaining safety and reliability of aircraft structures in the aerospace engineering industry. Similarly crucial insights related semiconductor materials characterizations are imperative for producing advanced electronic devices - microprocessors & memory chips being some examples- which fall under the purview of industries responsible for developing state-of-the-art electronic gadgets we use today.

Evaluating substances is a crucial step towards developing new materials and improving the current ones. This procedure furnishes a more profound comprehension regarding qualities and actions that are observed within substances, giving rise to fresh opportunities for scientists and engineers to craft ingenious technologies, as well as goods imbued with superior performance capabilities. For this research, spectrometer results of initial and final concentrations have been used to calculate the adsorption capacity of materials, XRD, SEM, EDAX, has been used to study how materials have behaved before and after adsorption. [18]

## 5.2. SPECTROPHOTOMETER

An instrument that is vital in evaluating and capturing color, the spectrophotometer makes use of two methods: transmission method which gauges how much light passes through an object; and reflectance process wherein a beam of light reflects off various visible spectrum wavelengths. Spectrophotometers are versatile tools capable of providing quantitative analysis for anything to ensure consistency from initial creation to final product delivery. These include but are not limited to liquids, plastics, metal, painted samples as well as cloth materials, among others.

The variety of spectrophotometers available makes it possible to choose one that suits any specific need. The device in question can measure light wavelengths at a certain angle, typically 45 degrees relative to the sample being evaluated. Although compact and highly effective against gloss interference, this type of spectrometer stands out for its ability to recreate how humans perceive colors. The beauty behind the 45:0 version lies in its mode of operation – with illumination occurring at an inclination equaling forty-five degrees from perpendicular as well as detection taking place without inclinations whatsoever (i.e., zero-degree angles). Regarding spherical types on offer, they have superior capacity when computing color measurements since

their reflectance capturing occurs not simply within regions but rather encompasses all sides simultaneously. UV-capable versions possess additional features beyond those mentioned above because besides facilitating measurement throughout various ultraviolet spectra ranges like non-UV models, i.e., these machines also allow users access into previously unreachable areas by probing deeper depths than before. Illumination happens uniformly or equally from every direction via such instruments while resultant reflected light registers upon detectors set up eight degrees apart after reflecting off surfaces under investigation - making them indispensable tools indeed.

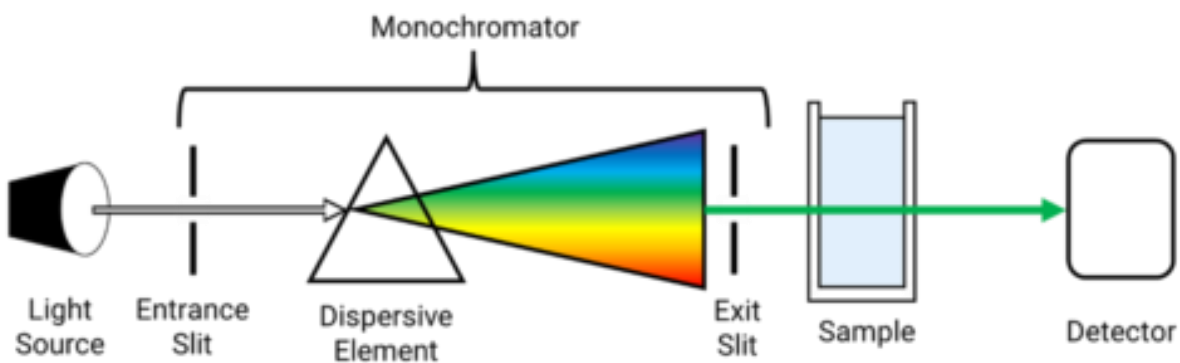


Figure 12, Spectrophotometer principle [11]

In a sphere spectrophotometer, the interior of the sphere is lined with a highly reflective, matte white material that is utilized to project and diffuse the light, creating a perfect white reflector. The color of a sample is seen by a multi-angle spectrophotometer. With up to twelve angles of measurement, the most recent multi-angle spectrophotometers can characterize, and measure effect finishes in a variety of applications, including automobile paint, plastics, and metals. In a twin beam spectrophotometer, the light intensity of two light paths—one carrying a reference sample and the other carrying a test sample—are compared. When a test sample is inserted, a

single-beam spectrophotometer compares the relative light intensity of the beam before and after.[10]



Figure 13, HACH D1900 portable spectrophotometer [12]

For this project, HACH portable DR 1900 spectrophotometer was used. The DR1900 is a light and portable spectrophotometer, making it ideal for use in the field. Moreover, it has the greatest range of test capabilities of any portable device. Almost 210 of the most widely used, preprogrammed methods are already included in the DR1900, which includes most of them. The user-friendly interface can be used to build custom methods as well. Also, it is adaptable since you can utilize the broadest range of vial sizes of any other spectrophotometer. The tests are conducted with a wavelength range of 340 to 800 nm, making this a field instrument which can be utilized to find results only seen in laboratory instruments. [12]

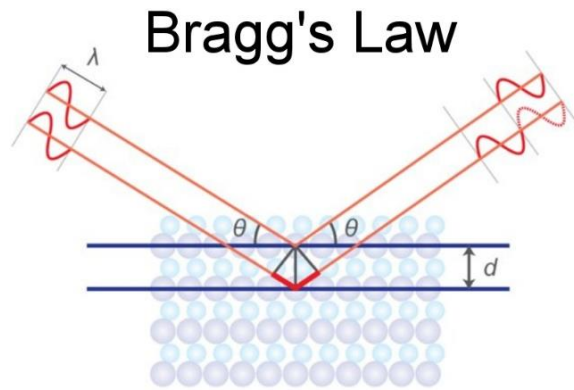
### 5.3. X-RAY DIFFRACTION

In crystallography involving X-rays, atoms arranged in a crystalline manner generate diffractions after being exposed to an incident X-ray beam which leads towards identifying atomic/molecular

structure respective to crystals at hand. By measuring angles and various intensities from said diffracted beams - it is possible to develop three-dimensional images reflecting electron density observed across these crystals themselves . The mean positioning for all atoms' sites is calculated alongside chemical bonds. Upon analysis of a sample utilizing the Powder XRD method, one can attain valuable information that complements and expands upon other microscopic or spectroscopic techniques. This includes recognizing phases present within samples, purity levels found therein as well as crystallite size when applicable to certain situations; occasionally morphology is also identified.

At its inception, crystallography was employed to ascertain the dimensions of atoms as well as characterize chemical bonds and atomic-level fluctuations in various materials. Minerals and alloys were given particular attention. For a singular X-ray diffraction measurement on a single-crystal specimen, researchers would attach it securely onto an apparatus known as a goniometer which allows for manipulation of angles between sample surfaces.

The crystal is illuminated by a focused beam of X-rays without any chromatic deviation to produce an evenly spaced pattern made up of spots. This reflection pattern, known as the diffraction pattern, is used alongside chemical data already gathered about the sample to transform two-dimensional images taken from different angles into a three-dimensional representation displaying electron density within the crystal via mathematical Fourier transforms.



$$n\lambda = 2d \cdot \sin\theta$$

Figure 14, X-Ray Diffraction Principle source: [www.rigaku.com/x-ray-diffraction-xrd](http://www.rigaku.com/x-ray-diffraction-xrd)

The upper left corner of the image above demonstrates how each scatterer reflects a small amount of the incoming beam's intensity as a spherical wave. In cases where the scatterers are evenly spread apart by a distance  $d$ , only certain directions will have  $2d \sin$  path-length changes that correspond to an integer multiple of wavelength  $d$ . A reflection zone shows up on the diffracting pattern whenever any portion of incoming light is diverted at a precise angle of two in identical circumstances. While destructive interference causes these waves to nullify each other out for most angles, they combine harmoniously within just a restricted handful as per Bragg's law - wherein  $n$  stands for integers and both  $\theta$  and  $\lambda$  stand respectively for incident angle and beam wavelengths while capital  $D$  denotes diffraction spacing between planes. Reflections are spots on the diffraction pattern that represent these directions. Therefore, an electromagnetic wave striking a regular array of scatterers causes X-ray diffraction.

When it comes to powder XRD, another application of this technology is phase identification. This approach typically involves comparing an experimental pattern with that of a reference pattern retrieved or generated from preexisting databases. Unfortunately, identifying phases

using XRD can be tricky when the diffraction patterns are identical - especially in nanoscale materials systems. Thankfully, there exist comprehensive powder diffraction databases available for purchase which serve as valuable resources and often come bundled alongside analytical software tools needed to analyze data obtained through experimentation. Moreover, some software packages allow direct simulation of these same patterns based on crystallographic information; other powerful features may include accounting for peak broadening due to nanocrystalline domains or preferred orientation effects during analysis.

An abundance of constituents that lack discernible XRD peaks relative to ambient noise can be noted among specimens with unfavorable signal-to-noise ratios, such as materials displaying weakly crystalline behavior and nanoscale matter featuring broadened peaks. Despite the necessity for supplementary experimental or computational techniques in blemish-free characterization, powder XRD provides insight into a range of pivotal attributes – including structure, phase composition, content distribution, morphology dimensions and purity measures - for samples exhibiting crystallographic domains at the nano level. [13]

#### 5.4. SCANNING ELECTRON MICROSCOPE

A particular kind of microscope, referred to as the scanning electron microscope or SEM for short, employs a focused beam of electrons for analyzing specimens and generating images. When an object is examined with this instrument, its atoms and electronic structure interact in such ways that produce numerous signals conveying details about both topographical features on the surface in question as well as chemical composition. The working involves maneuvering concentrated stream through different areas using a raster scan pattern while fusing all positions obtained from detected information into one picture.

As the scale of materials used for various purposes is reduced, scanning electron microscopes (SEMs) have emerged as powerful and versatile instruments for material analysis. Unlike light microscopes that rely on visible radiation to observe specimens, these use electrons to produce images. SEMs detect scattered or emitted electrons from near-surface regions of samples in contrast with transmission electron microscopes (TEMs), which utilize transmitted high-energy beams passing through thin slices of a specimen. The shorter wavelength of accelerated electrons compared to photons leads to greater resolution than available using optical microscopy techniques alone. SEM permits imaging at both extremely low temperatures and above ambient levels including under vacuum conditions such as wet environments without deterioration due to its diverse range capabilities.

When an electron beam stimulates atoms, secondary electrons are produced, and their measurement is taken. How the specimen's surface topography or the angle of incidence affects detection varies. A specialized detector captures emitted secondary electrons during sample scanning to generate a topographic image of its surface. Tungsten filament cathode-equipped electron guns emit thermionic beams in conventional SEMs because they can be electrically heated for emission without vaporizing due to their high melting point and low vapor pressure—all while remaining cost-effective compared with other metals used in similar applications.

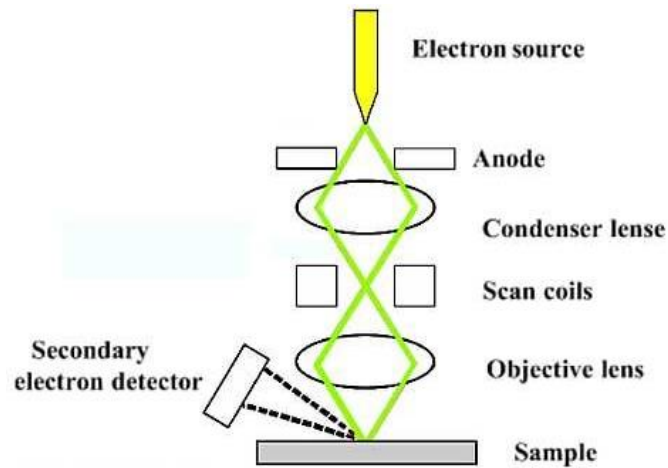


Figure 15, Scanning Electron microscope [14]

The fluctuation of electron beam energy ranges from 0.2 keV to 40 keV and is focused by one or two condenser lenses, creating a spot with diameter changing between 0.4 nm and 5 nm. Once the beam passes through scanning coils or deflector plates in the final lens column, it swerves unpredictably on both x-axis and y-axis. The interaction volume shaped like a teardrop under sample's surface stretches across dimensions ranging from 100nm up to five meters; this region indicates where primary electrons interact with samples causing sporadic scattering/absorption events that lead to loss of energy repeatedly overtime significantly accounting for most results sought after during testing.

The electron's landing energy is influenced by several factors including the specimen's atomic number, dimensions, and density. Other interactions between them can also be identified such as electromagnetic radiation produced from their exchange of energies while receiving beam currents absorbed in specialized detectors used to identify high-energy electrons and secondary electrons emanating from this interaction zone created upon contact. Furthermore, images capturing current conditions within specimens are taken through specific techniques using

uncommon scientific knowledge requiring significant expertise for full comprehension purposes.  
[14]

### 5.5. ELECTRON DISPERSIVE X-RAY ANALYSIS

An approach used to inspect elements present in a sample is Energy-dispersive X-ray spectroscopy, which can also be addressed as EDXA or EDX. This method utilizes x-rays with high-energy electromagnetic radiation that have the potential of eliminating electrons located inside an atom's nucleus region. In this technique, Moseley's Law was used which deduced the correlation between light frequency issued by objects and atomic number using electromagnetic radiation having higher energy levels than gamma rays emitted from radioactive substances such as uranium-238.

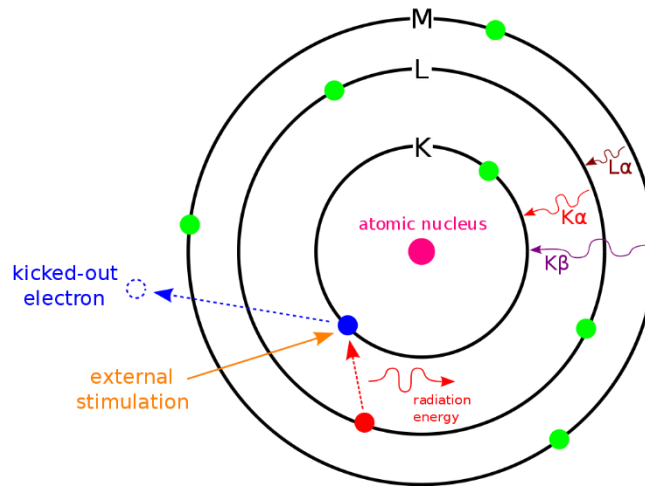


Figure 16, Principle of EDS [15]

An illustration of how EDS functions is provided above. While  $\alpha$  and  $\beta$  denote the size of the transition, K, L, and M refer to the n value that electrons in that shell have (K electrons, which are closest to the nucleus, are n=1 electrons). As a result, the transition from M to K would be

referred to as a K transition, as opposed to the relaxation from M to L or L to K. Siegbahn notation is the method utilized to represent these procedures.

The three main components of EDS are an emitter, a collector, and an analyzer. Moreover, these components are frequently installed on a SEM or TEM, two types of electron microscopes.

Combining these three components allows for examination of both the number of X-rays radiated and their energy (in comparison to the energy of the initial X-rays that were emitted).

The KeV and peak intensity of the EDS data are plotted on an x-y axis in a graph. A computer program converts the atoms that the energy changes represent at the highest place on the x-axis.

[15]

## 6. EXPERIMENTAL

### 6.1. KINETICS EXPERIMENTS

Kinetics experiments serve as a preeminent means for investigating the velocity at which substances adhere to surfaces. Adsorption posits that molecules and ions bind onto polar or non-polar surfaces via intricate mechanisms, including physisorption and chemisorption. The objective of kinetic investigations is to ascertain how factors such as temperature, pressure, as well as the composition of both adsorbent and adsorbate contribute to the rate at which such phenomena occur.

There exists a multitude of techniques to quantify the dynamics surrounding adsorption. A conventional strategy conveniently implemented is the deployment of a batch experiment, wherein an established quantity of adsorbate is titrated into an unchanging amount of adsorbent contained within a receptacle. The concentration gradient of said adsorbate can then be scrutinized at predetermined epochs, and subsequently evaluated for fluctuation over time to ascertain the rate of absorptive action underway.

An additional approach in the realm of adsorption experimentation is implemented through the usage of continuous flow experiments. This tactic involves a regulated stream of the target adsorbate being propelled throughout an anchored bed composed of various adsorbent materials, with measured concentrations procured at distinct points along its trajectory. After this data acquisition process, rates of adsorption are computed via assessments centered on variations in measuring degrees affiliated with gradients that occur as the adsorbed matter courses through the compacted bed.

In the methodology of both batch and continuous flow experimentation, the intricacies of adsorptive kinetics can be meticulously modeled by employing an array of distinct mathematical models, for example the Langmuir isotherm or the Freundlich isotherm. Delineating a connection between the concentration levels of an adsorbate substance and its corresponding amount that has been physically adsorbed on to the surface area of an adsorbent material; these models offer a sophisticated method at explicating through analysis what might have been previously obscured or confounding processes during scientifically controlled experiments.

The outcomes of kinetics experiments are indeed invaluable sources of information that may unravel crucial insights regarding adsorption processes, viz. the most suitable conditions for optimal adsorption, the intricate and dynamic nature of kinetics governing these processes as well as the potential adsorbent's ability to absorb a particular species known in scientific parlance as 'adsorbate'. This valuable knowledge can pave the way for optimizing designs and fine-tuning operations related to an assortment of applications including but not limited to water treatment, air purification, and gas separation mechanisms. [21]

#### **6.1.1. Chemicals required:**

- $\text{NaH}_2\text{PO}_4 \cdot 2\text{H}_2\text{O}$
- Distilled water
- Adsorbent (Activated Carbon, Basolite C300, Basolite Z1200, Basolite A100, Basolite F300, Basolite Z377)
- PhosVer 3 reagent powder

### **6.1.2. Equipment required:**

- Weighing scale
- Magnetic stirrer or Roller
- HACH DR1900 Spectrophotometer

### **6.1.3. Others**

- Filter paper
- Syringe
- Vial
- Nalgene container

### **6.1.4. Procedure**

- 1.642 grams of  $\text{NaH}_2\text{PO}_4 \cdot 2\text{H}_2\text{O}$  was weighed and added to 1000ml of distilled water and mixed well until it was dissolved. Theoretically, the solution should have a concentration of 2mg/L.
- The pH of the solution was measured. Three different pHs 5, 7, and 9 were used in this research. The pHs were adjusted using Sodium hydroxide (NaOH) and Hydrochloric Acid (HCl).
- The concentration of the solution was checked using the HACH DR1900 spectrophotometer. The inbuilt '490p react PV' program was used where the visible light of 710nm passed through the sample. The concentration should be under 2.50mg/L since that is the maximum measurement for that program. To check the concentration of the solution, it needed to be diluted. So 20 $\mu$ l of solution was mixed with 10ml of distilled water.

- Then 100ml of solution was taken in a separate container.
- **1 gram** of the adsorbent is measured and added to the container having 100ml solution.
- The container was kept in a magnetic stirrer or a roller at 200rpm for 24 hours.
- Every hour 3ml of solution was taken in a syringe, filtered into a vial, and stored.
- The sample was taken at 1, 2, 3, 4, 5, 6hrs and then at 24-hour and stored for spectrometer experiments.
- At the end of 24 hours, the entire solution was filtered, and the adsorbent was dried out using vacuum chamber and stored for characterization.



Figure 17, General Procedure of Adsorption Experiments. Source: “Created with

[BioRender.com](https://www.biorender.com).”

## 6.2. ISOTHERM EXPERIMENTS

Isotherm experiments play a pivotal role in adsorption studies, serving as an intrinsic tool in assessing the interactions between adsorbate molecules and surface-laden solid materials. In its very essence, an isotherm serves to depict, graphically, the interconnection existing between the quantity of adsorbate that is immobilized upon an adsorbent's surface and the level of equilibrium concentration for adsorbate within either the gas or liquid phases. The temperature maintained during testing is considered constant.

The process entails introducing a fixed quantity of gas or liquid elixir that contains the adsorbate onto the exterior of this material we term the 'adsorbent material.' Following this setup, intensity measurements are conducted at multiple equilibriums levels to determine with accuracy and thoroughness how much amount they have pressed on said adsorbent material. The data procured through said experiments can then be formulated into diverse kinds of guidelines such as adsorption isotherms, which give a solid understanding regarding two facets about these adsorbents, firstly their ability to be held by diverse surfaces and secondly just how potent those surfaces happen to be.

Numerous types of adsorption isotherms are typically utilized during isotherm experiments. These include Langmuir, Freundlich, and BET isotherms. The Langmuir isotherm operates under the assumption that the adsorption process is monolayered, whereupon once adsorbate molecules have been taken up by the surface, they no longer interact with each other. In contrast to this, the Freundlich isotherm supposes multilayered processes occurring whereupon adsorbed items decrease in strength as concentration increases. As for the BET isotherm model, it incorporates a

more intricate approach by accounting for both monolayer and multilayer instances in combination; frequently applied for encompassing porous material adsorption behavior studies.

Undertaking isotherm experiments can offer crucial data concerning the adsorption conduct of diverse absorbent materials, enabling their practical applications in fields like gas purification, water treatment, and catalysis. By comprehending material adsorption behavior, researchers may create more proficient and compelling absorbents catered to usage scenarios; with a synchronized intensity that reflects genuine situations in our world. [22]

### **6.2.1. Freundlich Isotherm**

The Freundlich isotherm model is extensively utilized in the field of adsorption studies to expound the correlation between the adsorbed quantity of adsorbate molecules onto an adsorbent surface, with regards to both gas and liquid phase concentrations of said molecules at a specific temperature. Herbert Freundlich originally proposed this model back in 1906, presuming that it was multilayered in its operation.

The Freundlich isotherm can be mathematically articulated in the following manner:

$$q = K_f * C_e^{1/n}$$

To gauge adsorption, a comparison of the quantity of adsorbate that has been taken up by the adsorbent against the mass of said adsorbent must be analyzed. Additionally, it is crucial to reference both  $C_e$  - which represents the stability reach within the gas or liquid phase- and  $K_f$ ; a constant linked with an adsorbent's capacity for absorbance. In contrast, the letter N denotes not

only the unevenness present in a substance's adsorbency properties, but also its capacity for capturing approaching particles.

The Freundlich exponent, represented by the symbol 'n,' serves as a critical determinant of adsorbent attraction capacity, fluctuating within the range of 0 to 1. In cases where n equals one, an adsorption process occurs in a uniform and straightforward pattern. Conversely, when n is less than 1, the adsorption strength dwindles with an increase in the concentration of the adsorbate substances present. Similarly, for instance when n surpasses one; this signifies that there tends to be higher adsorption potency managed through an escalation in adsorbate chemical composition.[23]

The Freundlich isotherm presupposes that the adsorption process is not ideal, which implies that the molecules of the adsorbate interact with one another after being secured to the surface. This model can be sparingly applied across a broad array of suitable substances, including those which have heterogeneous and porous structures.

The eminent Freundlich isotherm holds a prominent place in the realm of environmental systems, especially when it comes to capturing pollutants from both air and water. Researchers also utilize this isotherm for developing adsorbent materials utilized for various industrial processes ranging from catalysis and chromatography to gas purification. A deeper comprehension of differing materials' adsorption nooks-and-crannies enables scientists to improve their efficiency in real-world situations while fabricating more efficient as well as effectual adsorbents tailored specifically for certain purposes. [24]

#### 6.2.1.1. Procedure

- 1.642 grams of  $\text{NaH}_2\text{PO}_4 \cdot 2\text{H}_2\text{O}$  was weighed and added to 1000ml of distilled water and mixed well until it was dissolved.
- The pH of the solution was measured. Three different pHs 5, 7, and 9 were used in this research. The pHs were adjusted using Sodium hydroxide (NaOH) and Hydrochloric Acid (HCl).
- The concentration of the solution was checked using the HACH DR1900 spectrophotometer. 20 $\mu\text{l}$  of solution was mixed with 10ml of distilled water.
- Then 100ml of solution was taken in a separate container.
- **0.5 gram** of the adsorbent is measured and added to the container having 100ml solution.
- The container was kept in a magnetic stirrer or a roller at 200rpm for 2weeks.
- The sample was taken at 1, 3, 7 and then at 14 days and stored for spectrometer experiments.
- 3ml of solution was taken in a syringe, filtered into a vial, and stored.
- At the end of 2 weeks, the entire solution was filtered, and the adsorbent was dried out using vacuum chamber and stored for characterization.

## 7. RESULTS AND DISCUSSION

### 7.1. ADSORPTION KINETICS

#### 7.1.1. Spectrometer Results and Adsorption Capacity

Following the experiment, the collected samples were subjected to spectrometer evaluation.

HACH DR1900 spectrophotometer was used. Since the spectrometer has a maximum limit of measuring up to 2.50mg/L, 20 $\mu$ L solution was diluted in 10ml for the spectrophotometer experiments so that the theoretical value of phosphate in the solution would be 2.0mg/L.

The initial concentration of the solution with pH 5 was measured to be 2.21mg/L. Table 1 has the spectrophotometer values of the concentration of the solution at pH 5 after 24 hours. The spectrometer values were then converted to a 1000ppm value by simply multiplying it by 500.

The capacity was calculated using the formula:

$$Capacity = \frac{((initial\ conc - final\ conc)mgL^{-1} * Volume\ L)}{Weight\ of\ absorbent\ g}$$

pH 5 -KINETICS									
Spectrometer reading	Time 0hr	1hr	2hrs	3hrs	4hrs	5hrs	6hrs	24hrs	Capacity (mg/g)
Activated Carbon	2.21	2.19	2.15	2.11	2.08	2.04	1.99	1.94	<b>13.40</b>
Basolite C 300	2.21	2.17	2.13	2.11	2.07	2.06	2.04	1.99	<b>10.97</b>
Basolite Z 1200	2.21	2.05	2.02	1.96	1.92	1.86	1.84	1.82	<b>19.48</b>
Basolite A 100	2.21	1.37	1.23	1.11	0.93	0.85	0.81	0.28	<b>96.38</b>
Basolite F 300	2.21	1	0.95	0.82	0.72	0.68	0.59	0.55	<b>82.81</b>
Basolite Z 377	2.21	0.2	0.19	0.17	0.13	0.11	0.09	0.07	<b>106.47</b>

Table.1, Spectrophotometer readings of pH 5 and the calculated capacity

The capacity of Basolite A100, Basolite F300, and Basolite Z377 were comparatively better than capacity of Activated Carbon, Basolite C300 and Basolite Z1200. From the graph it is also noticeable that the three adsorbents which have better capacity also have a sudden drop in concentration after just 1 hour. Fig. 17 shows how the adsorbents have reacted to the phosphate solution in 24 hours. Interestingly, Basolite C300 which has efficiently worked in Nitrogen adsorption has lesser potential than Activated Carbon in phosphate adsorption. Also, during the experiment it was evident that Basolite Z377 and Z1200 were completely soluble in the solution where rest of them were non soluble.

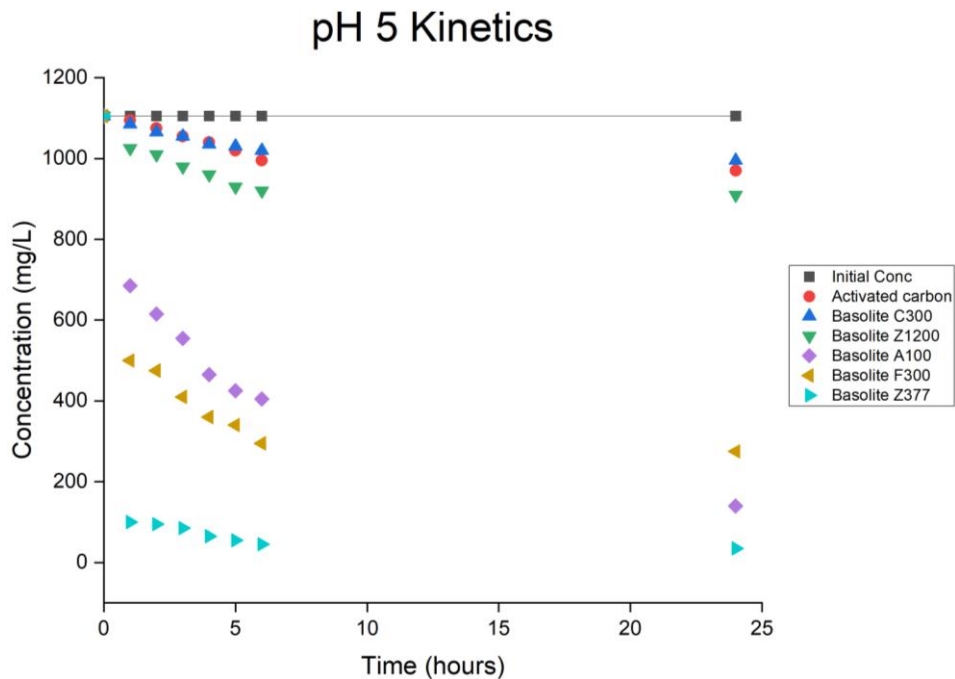


Figure 18, Concentration Vs Time, Kinetics graph of pH 5

Likewise for pH 7, the initial concentration of the solution with pH 7 was measured to be 2.11mg/L. Table.2, has the spectrophotometer values of the concentration of the solution at pH 7 after 24 hours.

pH 7 - KINETICS									
Spectrometer reading	Time (hr.) 0	1hr	2hrs	3hrs	4hrs	5hrs	6hrs	24hrs	Capacity (mg/g)
Activated Carbon	2.11	2.09	1.98	1.96	1.9	1.85	1.81	1.54	<b>28.47</b>
Basolite C 300	2.11	2.11	2.1	2.07	2.05	2.05	1.98	1.77	<b>16.98</b>
Basolite Z 1200	2.11	1.35	1.34	1.33	1.31	1.28	1.28	1.27	<b>41.96</b>
Basolite A 100	2.11	1.36	1.32	1.15	1.01	0.97	0.85	0.26	<b>92.45</b>
Basolite F 300	2.11	1	0.96	0.92	0.86	0.85	0.82	0.78	<b>66.43</b>
Basolite Z 377	2.11	0.32	0.26	0.22	0.17	0.14	0.14	0.14	<b>98.42</b>

Table.2, Spectrophotometer readings of pH 7 and the calculated capacity

At the end of pH 7 experiments, it is apparent that the Activated carbon and Basolite Z1200 has better capacity value when compared with pH 5, while Basolite F300 capacity was lesser than pH 5 meaning that Activated Carbon and Basolite Z1200 performed better at pH 7 while Basolite F300 performed better at pH 5 solution. The other adsorbents such as Basolite C300, A100, and Z377 performed similar at both pH 5 and pH 7.

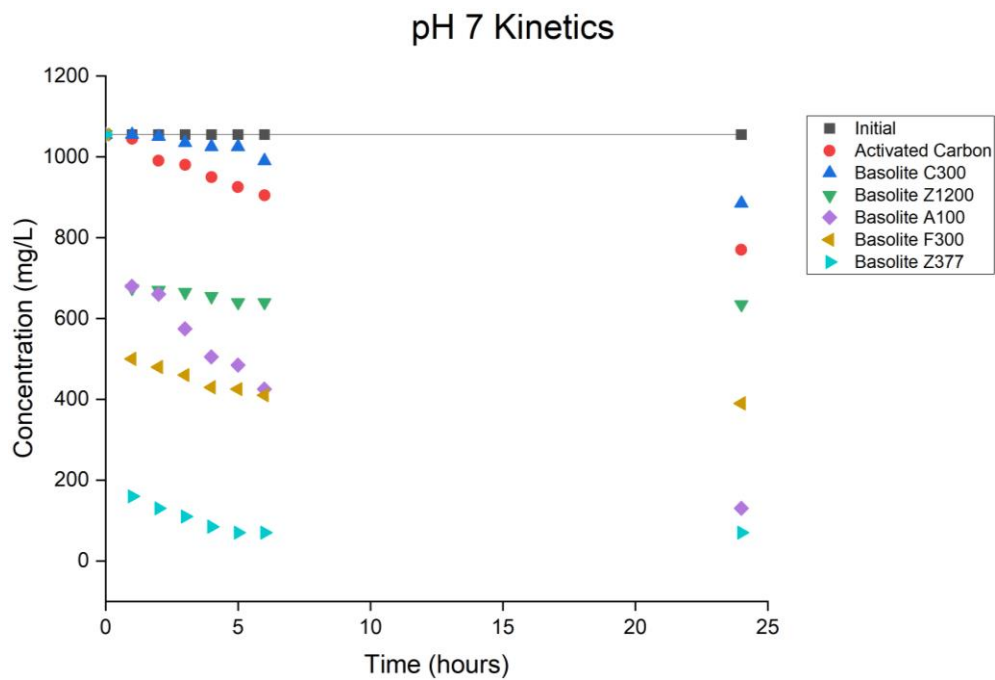


Figure 19, Concentration Vs Time, Kinetics graph of pH 7

Correspondingly, at pH 9 the initial concentration of the solution was measured to be 2.27mg/L.

Table.3, has the spectrophotometer values of the concentration of the solution at pH 9 after 24 hours.

<b>pH 9 - KINETICS</b>									
<b>Spectrometer reading</b>	<b>Time (hr) 0</b>	<b>1hr</b>	<b>2hrs</b>	<b>3hrs</b>	<b>4hrs</b>	<b>5hrs</b>	<b>6hrs</b>	<b>24hrs</b>	<b>Capacity (mg/g)</b>
Activated Carbon	2.27	2.24	2.21	2.15	2.11	2.07	2.06	2.02	<b>12.47</b>
Basolite C 300	2.27	2.23	2.19	2.09	2.07	2.04	1.99	1.96	<b>15.43</b>
Basolite Z 1200	2.27	2.17	2.1	2.07	2.05	2.02	1.98	1.93	<b>16.97</b>
Basolite A 100	2.27	1.71	1.17	0.96	0.88	0.74	0.68	0.07	<b>109.74</b>
Basolite F 300	2.27	0.76	0.69	0.62	0.49	0.46	0.44	0.38	<b>94.26</b>
Basolite Z 377	2.27	0.18	0.1	0.09	0.07	0.06	0.05	0.04	<b>111.23</b>

Table.3, Spectrophotometer readings of pH 9 and the calculated capacity

It is observed that at pH 9, Basolite A100 and Basolite F300 capacity results were better than pH 5 and pH 7. Basolite Z1200 and Activated carbon show equivalent results compared to pH 5.

Basolite Z377 and Basolite C300 results were similar in all three pHs.

In conclusion, Basolite Z1200 and Activated carbon work well at pH 7 wherein Basolite A100 and F300 work well at pH 9. Basolite Z377 and Basolite C300 work the same in all pHs. Overall Basolite Z377 possesses the highest adsorption capacity than other adsorbents.

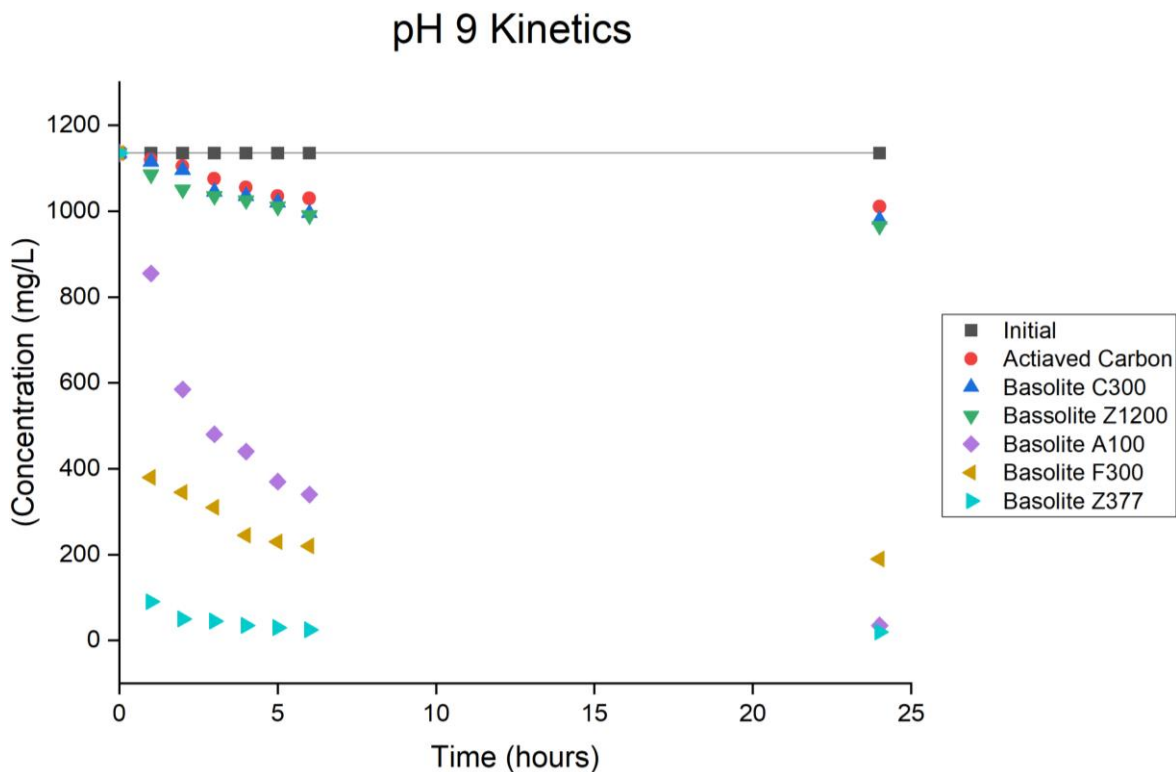
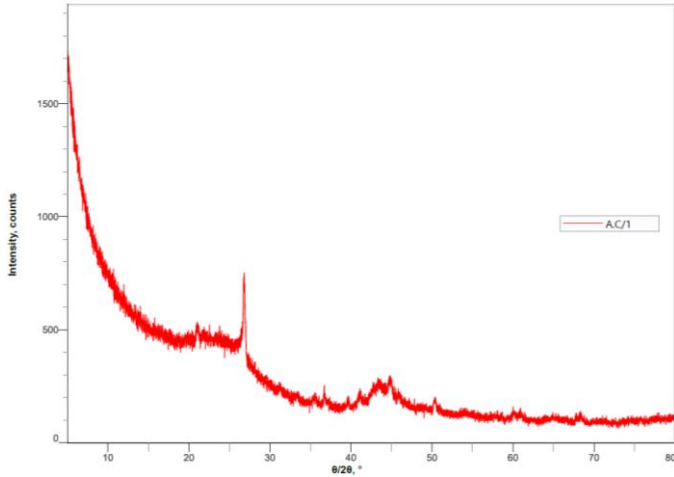


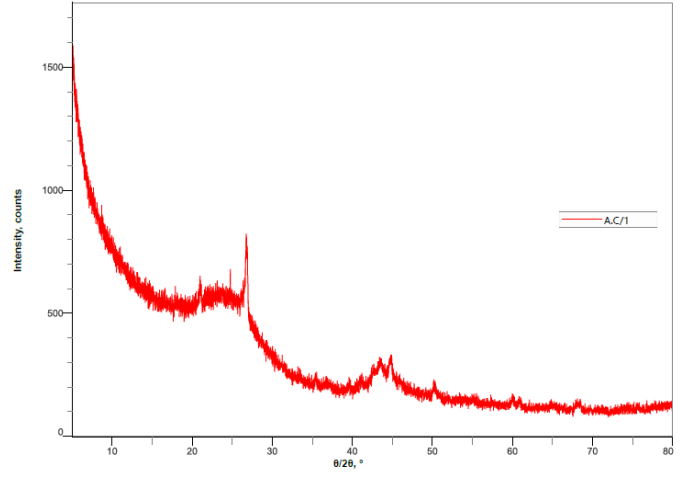
Figure 20, Concentration Vs Time, Kinetics graph of pH 9

### 7.1.2. X-Ray Diffraction

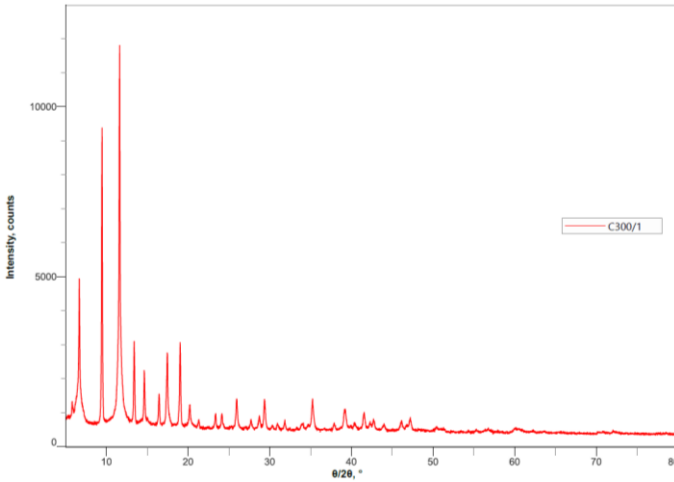
X-Ray Diffraction was done at Wright State using Rigaku XRD machine and Rigaku's Smart Lab Studio II software was used to run the machine. The data was saved as individual projects. The X-ray of 40kV voltage and 30mA current was used. The X-Ray source of Cu-K $\alpha$  with 1.54186Å wavelength was used. Following is the XRD graph of both before and after treatment (pH 5) compared. Comparing the graphs, it is obvious that there was not much change in the graph except for some noise in the after-treatment graphs. From this we can conclude that the phosphate adsorption did not affect the existing crystal structure or its crystallinity property. pH 7 and pH 9 had similar graphs as well.



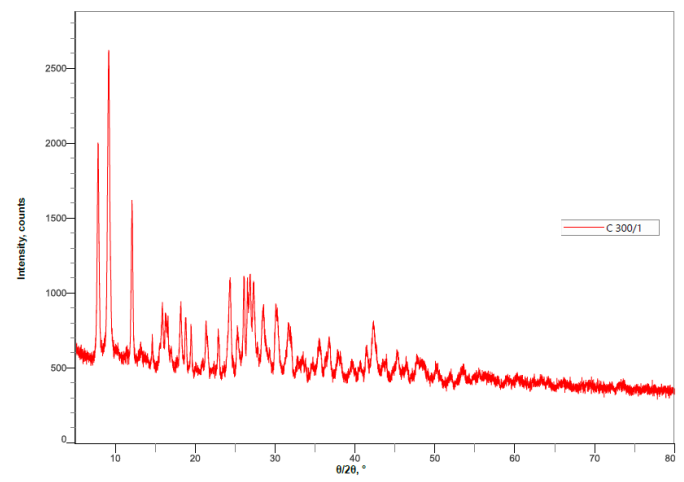
a) Before Treatment - Activated Carbon



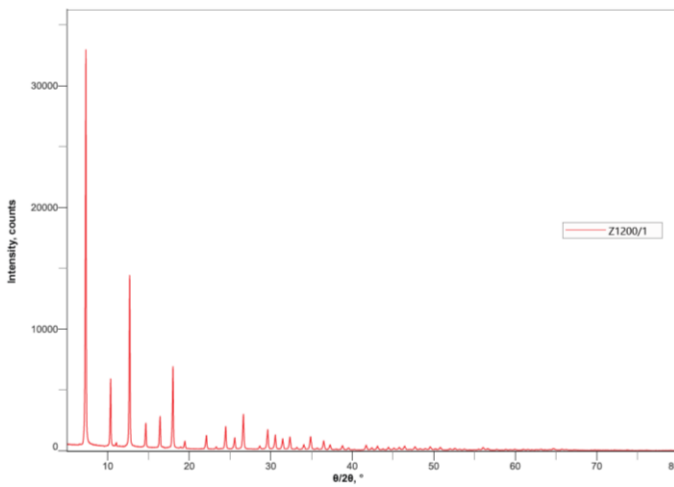
b) pH 5 – Activated carbon



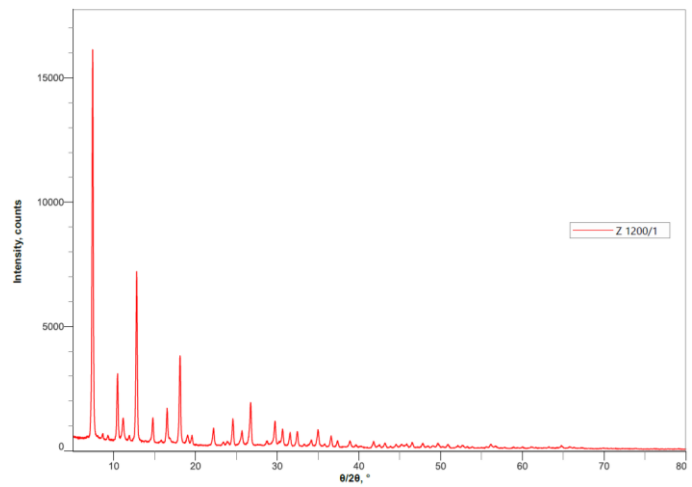
c) Before Treatment - Basolite C300



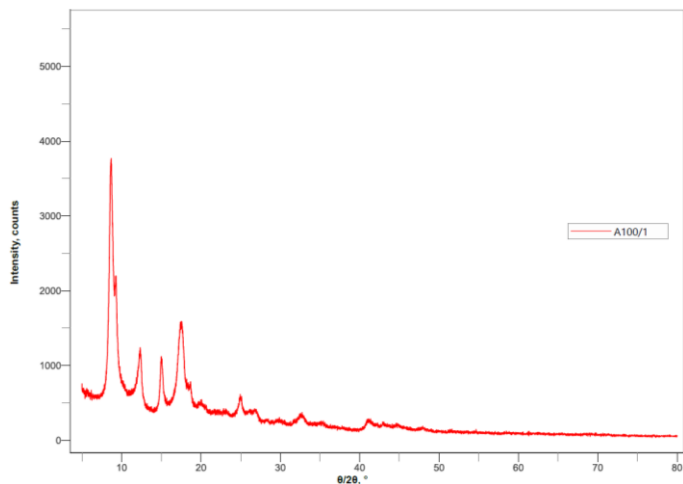
d) pH 5 – Basolite C300



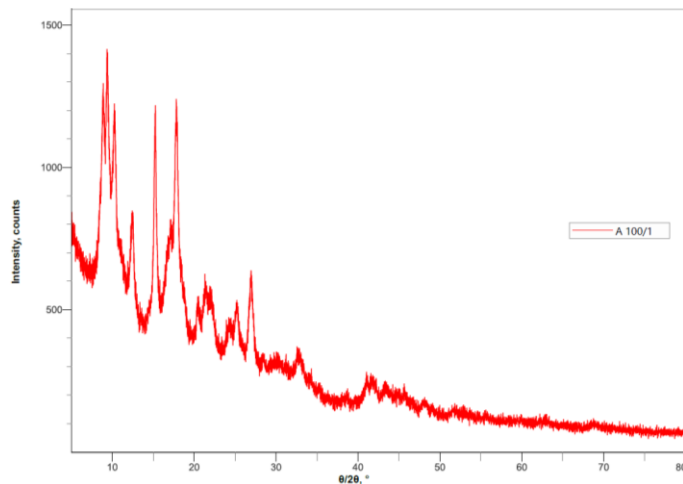
e) Before Treatment - Basolite Z1200



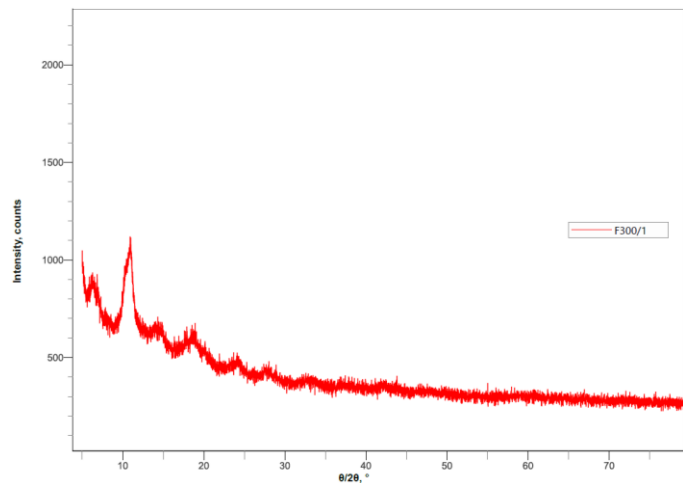
f) pH 5- Basolite Z1200



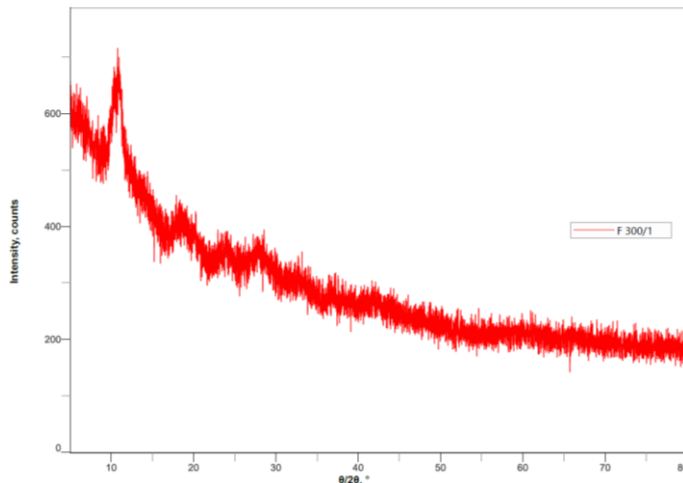
g) Before Treatment - Basolite A100



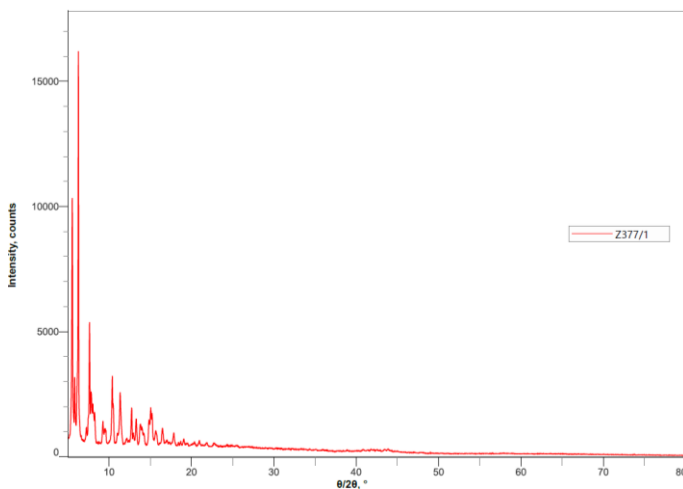
h) pH 5 – Basolite A100



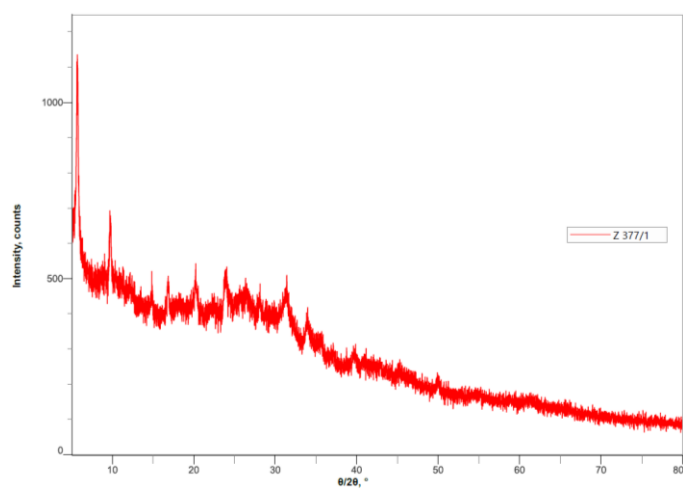
i) Before Treatment - Basolite F300



j) pH 5 – Basolite F300



k) Before Treatment – Basolite Z377

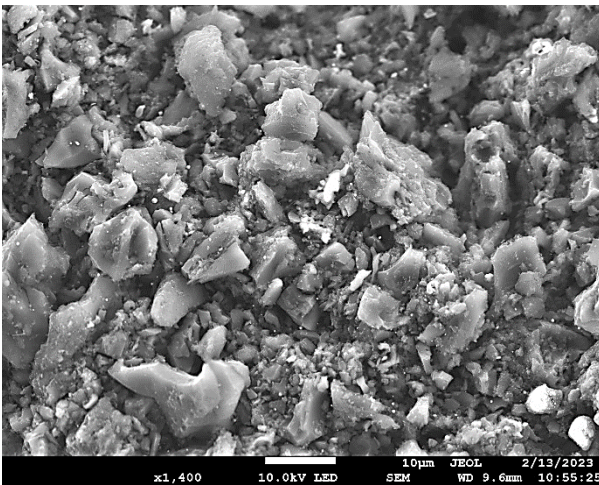


l) pH 5 – Basolite Z377

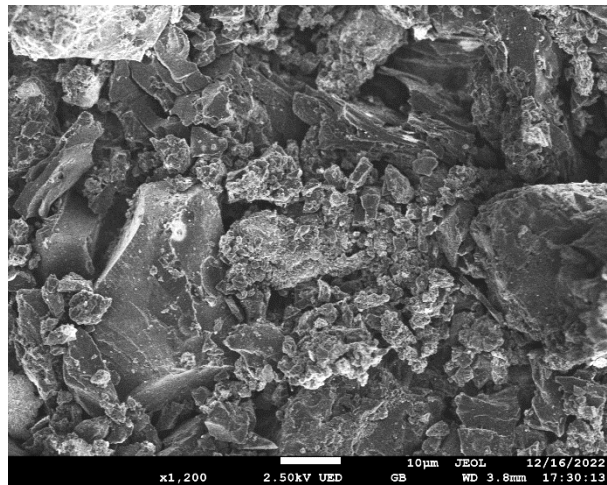
Figure 21, XRD images of the adsorbents before and after adsorption.

### 7.1.3. SEM Images

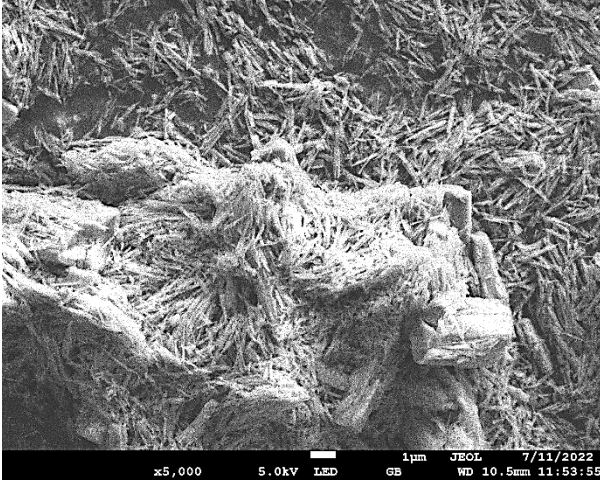
SEM images were taken using JEOL FEM-SEM (Field Emission Microscope) at Wright State. The vacuum dried samples after 24 hours were assessed. Working distance ranging from 3-10mm was used for the samples. The samples were charged up easily so Gentle Beam (GB) was passed to the sample, where the number of electrons from source was refined and limited. Also, UED (Upper Electron Detector) was used. The voltage of about 2.5kV – 12kV was used based on the sample. From observing before and after treatment samples, The SEM images of Basolite C300 before treatment looked like continuous flakes at 5000X and Basolite C300 after treatment looked like smaller flakes at 15,000X. Basolite Z1200, Basolite A100, Basolite Z377 and Basolite F300 structures before and after treatments resembles clusters like structures. The following images are the SEM images of adsorbents in as bought condition and after 24 hours of treatment at pH 7. The SEM images after treatment looked similar for pH 5 and pH 9.



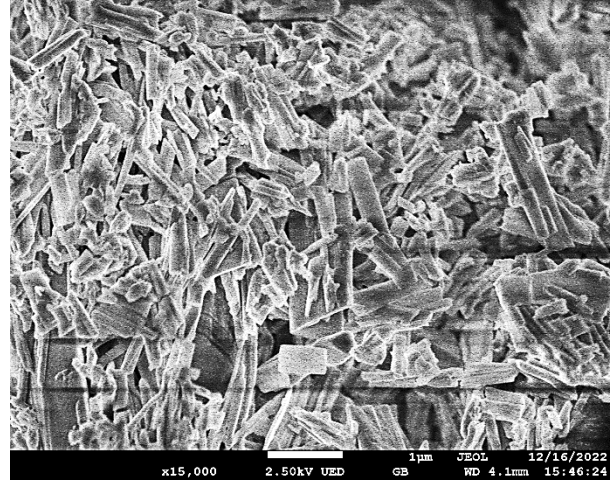
a) Before Treatment – Activated Carbon



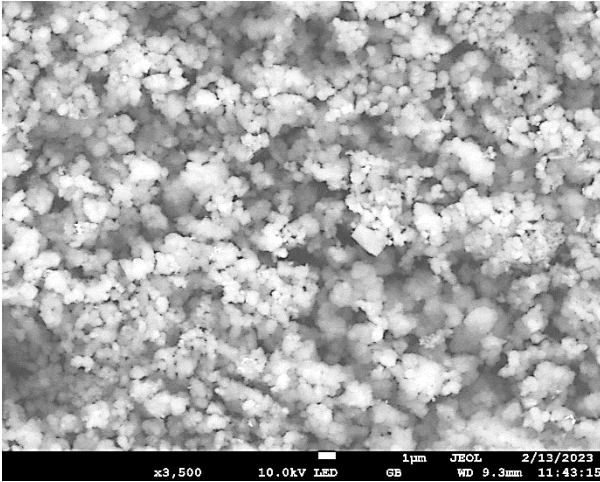
b) pH 7 – Activated Carbon



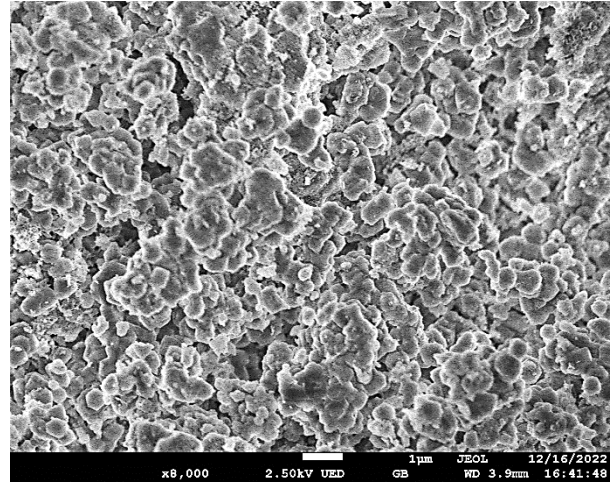
c) Before Treatment – Basolite C300



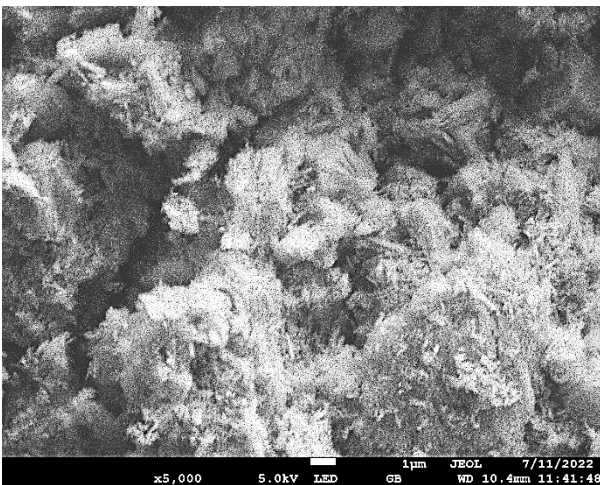
d) pH 7 – Basolite C300



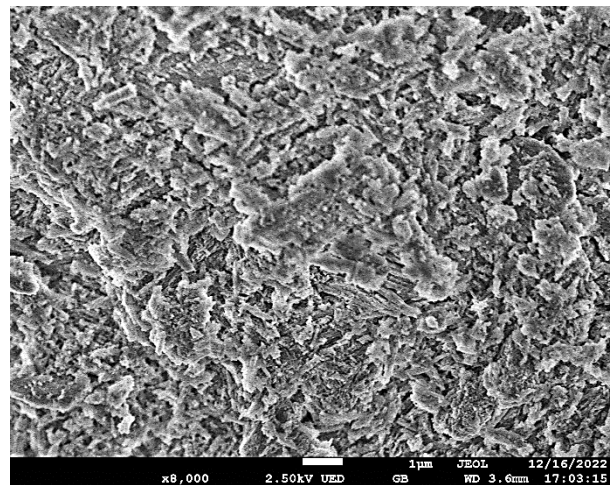
e) Before Treatment – Basolite Z1200



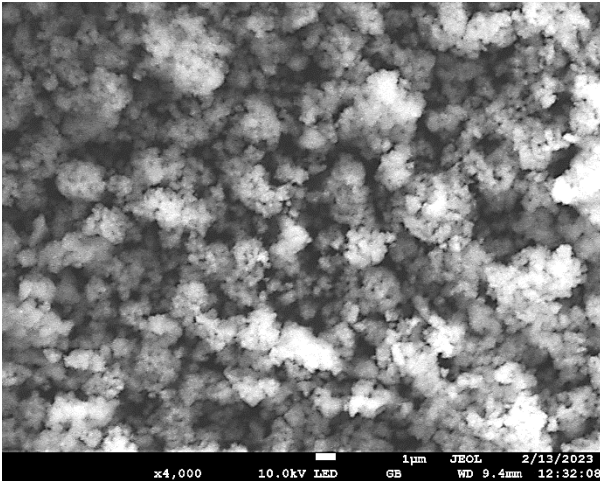
f) pH 7 – Basolite Z1200



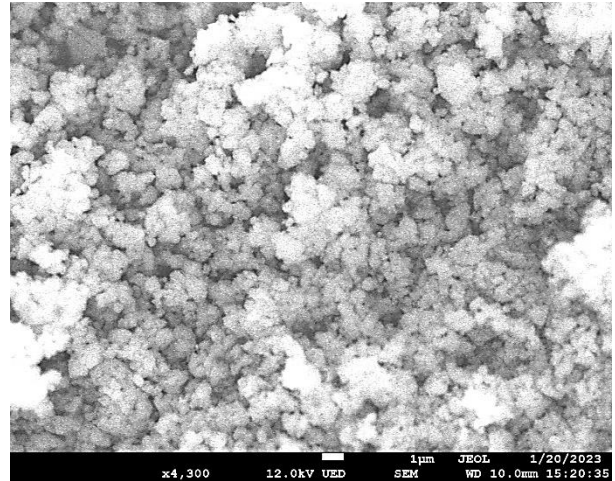
g) Before Treatment – Basolite A100



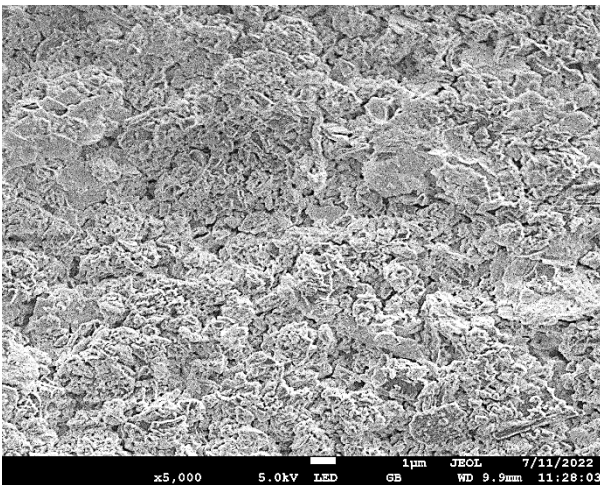
h) pH 7 – Basolite A100



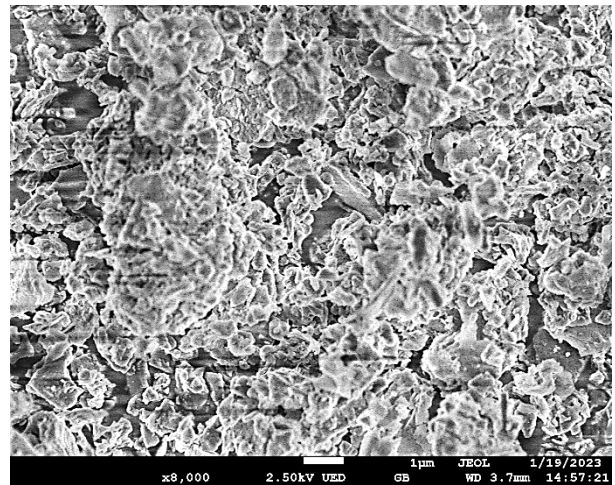
i) Before Treatment – Basolite F300



j) pH 7 – Basolite F300



k) Before Treatment – Basolite Z377



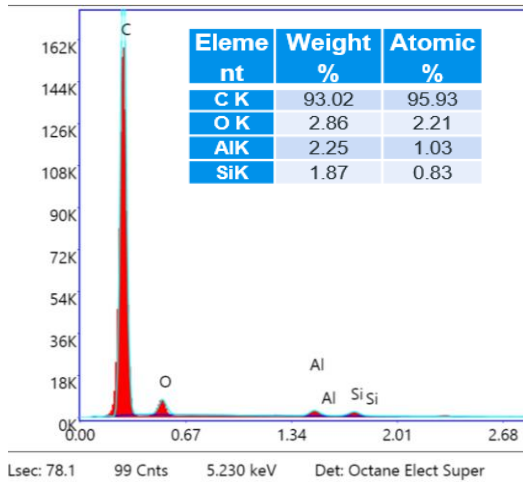
l) pH 7 – Basolite Z377

Figure 22, SEM images of the adsorbents before and after adsorption.

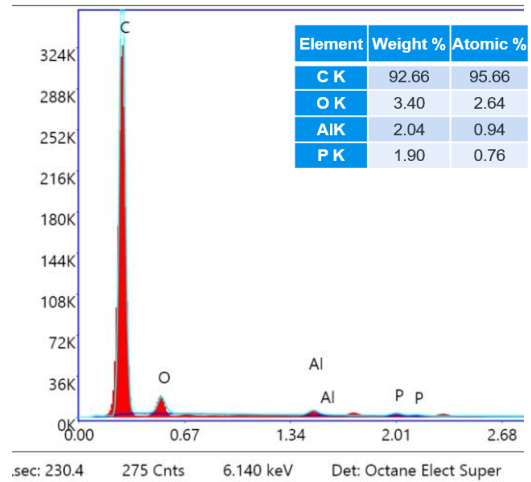
#### 7.1.4. EDS Results

Energy Dispersive Spectroscopy was done at Wright State. For EDS, EDAX system connected with SEM was used. EDS data provides the weight and atomic percentage of elements on the sample. Mapping was done at three distinct locations in each sample. It is evident that the “as bought” adsorbent has no presence of phosphorus while the after-treatment data shows presence of phosphorus. The images below show the comparison between before and after treatment of

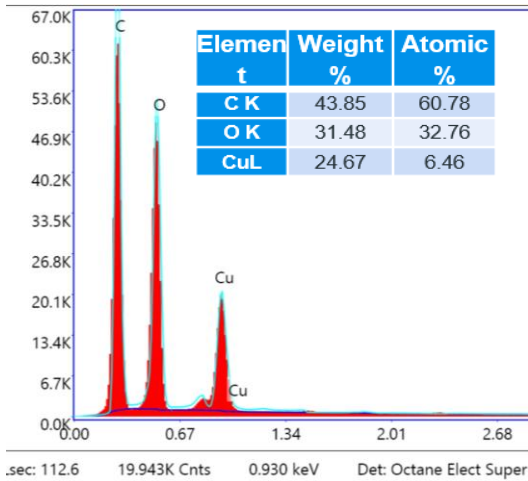
the adsorbents. It was observed that the phosphorus value changes at different spots in the sample but the changes in value were unwavering.



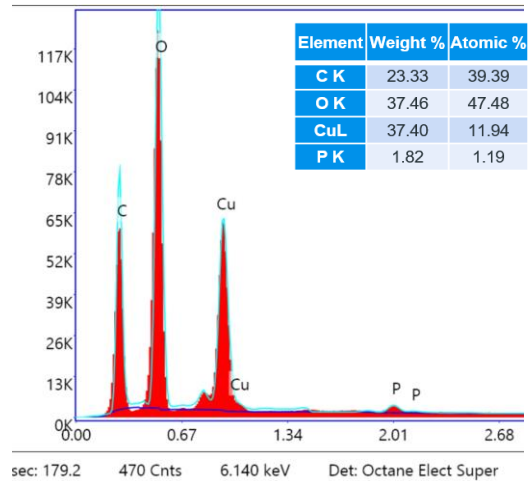
a) Before Treatment – Activated Carbon



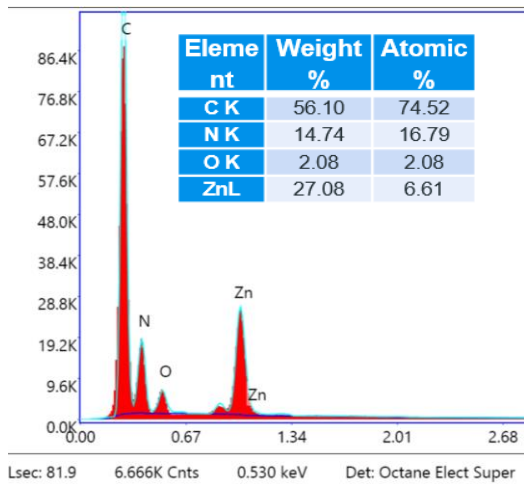
b) pH 5 – Activated Carbon



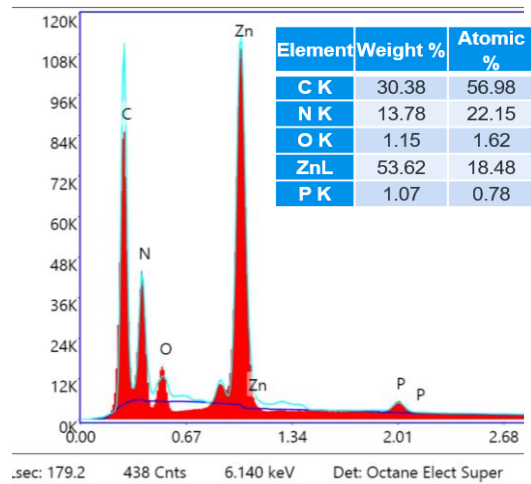
c) Before Treatment – Basolite C300



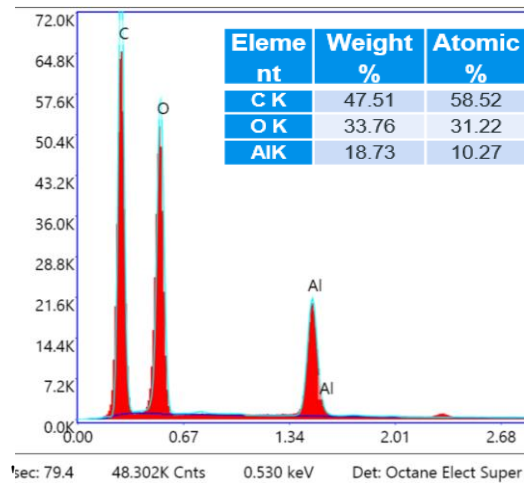
d) pH 5 – Basolite C300



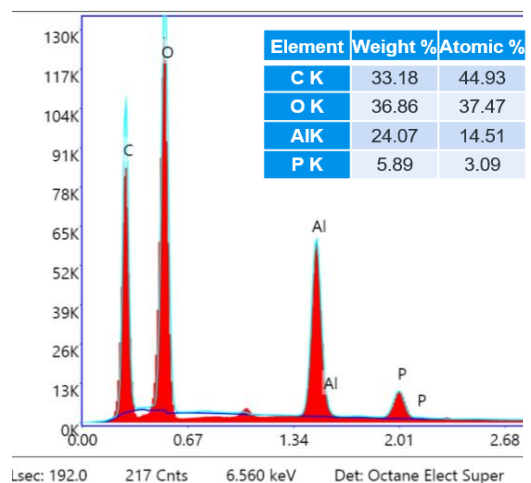
e) Before Treatment – Basolite Z1200



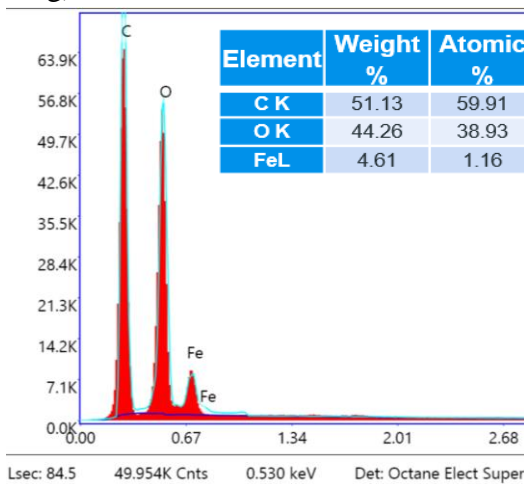
f) pH 5 – Basolite Z1200



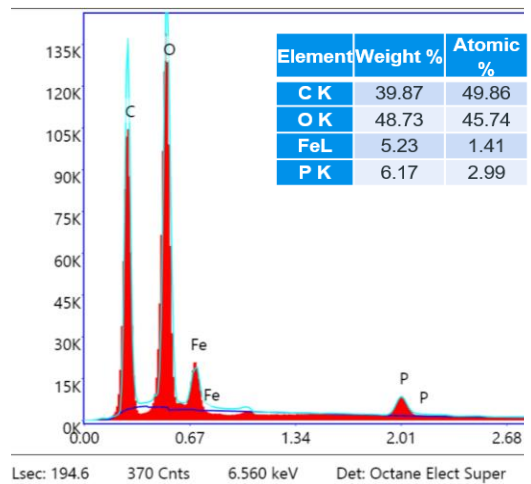
g) Before Treatment – Basolite A100



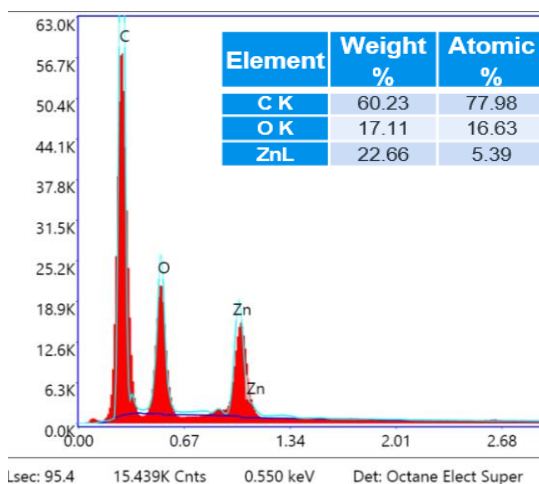
h) pH 5 – Basolite A100



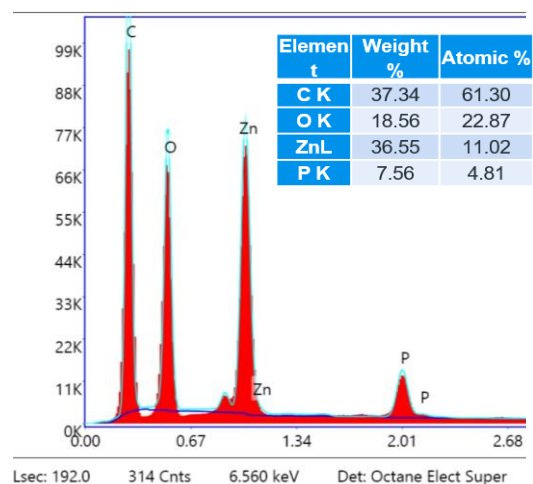
i) Before Treatment – Basolite F300



j) pH 5 – Basolite F300



k) Before Treatment – Basolite Z377



l) pH 5 – Basolite Z377

Figure 23, EDAX graph of the adsorbents before and after adsorption.

### 7.1.5. TEM and STEM

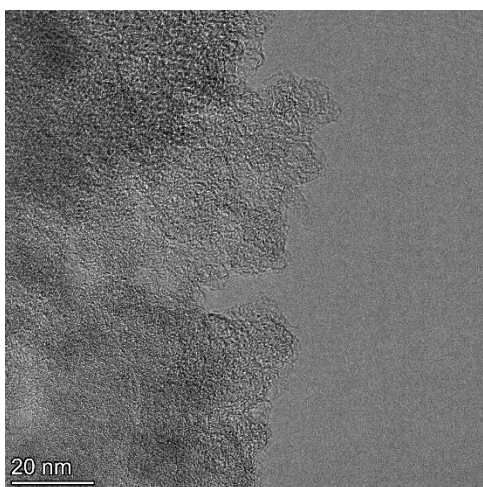
TEM (Transmission Electron Microscope) and STEM (Scanning Transmission Electron Microscope) analysis was done for the adsorbents. TEM was done at the University of Kentucky with the help of EPA and STEM was done at Wright State’s SEM facility. Transmission electron microscope (TEM) deploys an electron beam for visualizing the atomic structure of materials. TEM operates by transmitting high-energy electrons through samples that are typically less than 100 nanometers in thickness, allowing for detailed analysis of their internal structure.

The specimen is situated on a unique sample holder, and the electron beam is targeted onto it by means of an array of electromagnetic lenses. Transmission electron microscopes can produce clear visuals with resolutions of up to 0.1-0.2 nanometers which is superior to the constraints posed by optical microscopy techniques.

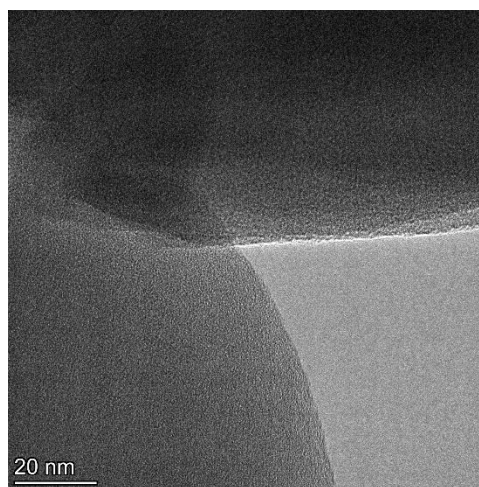
STEM (Scanning Transmission Electron Microscope) employs a focused beam of electrons and offers detailed images of sample surfaces unlike traditional TEMs which pass through samples to

generate an image. The electron beam participates in interactions with atoms and molecules comprising it, resulting in a myriad of signals that can be identified by detectors equipped within STEM. The transmitted electrons as well as scattered electrons deflected off samples was captured by detectors.[28]

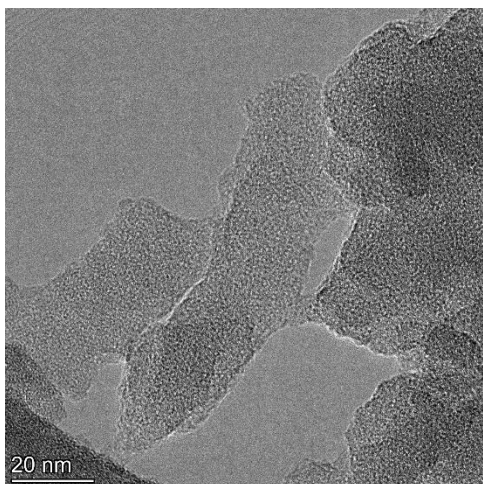
The phases are not visible clearly, from this we can conclude that the particles are large. The particles are thicker making it difficult for the electrons to pass through.



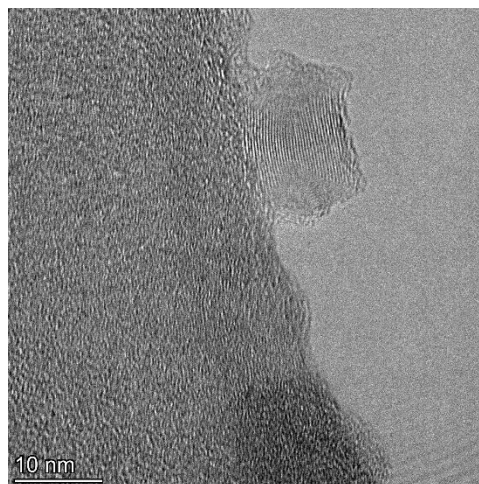
a) Activated Carbon



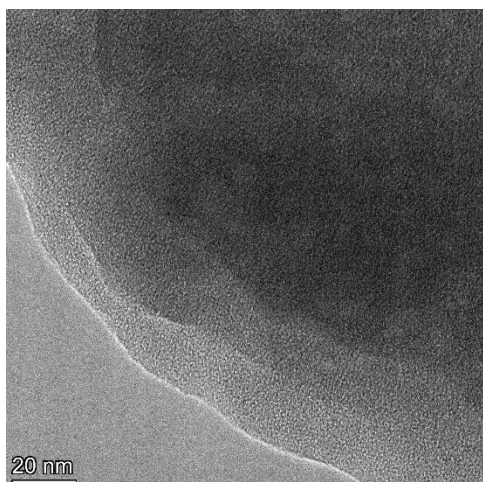
b) Basolite Z1200



c) Basolite A100



d) Basolite F300



e) Basolite Z377

Figure 24, TEM images of the adsorbents after adsorption.

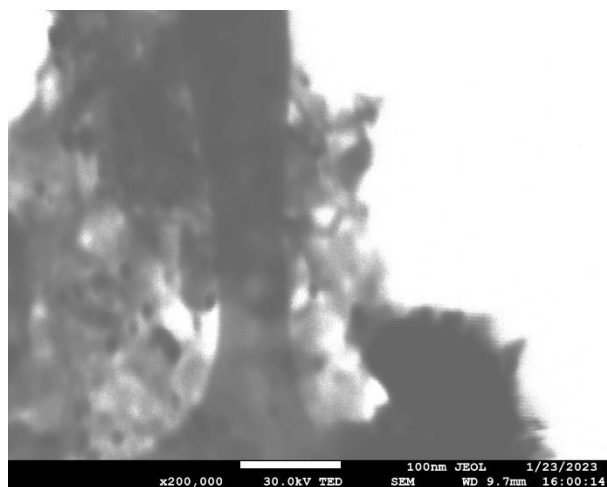


Figure 25, STEM image - Basolite Z1200

## 7.2. ADSORPTION ISOTHERM

### 7.2.1. Spectrometer Results and Adsorption Capacity

Following the 14-day experiments, the collected samples were subjected to spectrometer evaluation. The initial concentration of the solution with pH 5 was measured to be 2.40mg/L. The spectrometer values were then converted to a 1000ppm value by simply multiplying it by

500. Table 4 shows the spectrophotometer values of the concentration of the solution at pH 5 after 14 days.

<b>pH 5</b>						
<b>Spectrometer reading</b>	<b>Time Day 0</b>	<b>Day 1</b>	<b>Day 3</b>	<b>Day 7</b>	<b>Day 14</b>	<b>Capacity (mg/g)</b>
Activated Carbon	2.4	2.28	2.09	2.02	2.01	<b>38.81</b>
Basolite C 300	2.4	2.33	2.2	2.16	2.12	<b>27.77</b>
Basolite Z 1200	2.4	2.38	1.99	1.68	1.12	<b>126.56</b>
Basolite A 100	2.4	1.54	1.32	1.03	0.55	<b>184.41</b>
Basolite F 300	2.4	1.41	1.38	1.34	1.25	<b>114.63</b>
Basolite Z 377	2.4	1.02	0.7	0.63	0.61	<b>178.22</b>

Table.4, Spectrophotometer readings of pH 5 after 14 days and the calculated capacity

The capacity of Basolite A100, Basolite F300, and Basolite Z377, Basolite Z1200 were comparatively better than capacity of Activated Carbon, and Basolite C300. Fig. 23 shows how the adsorbents have reacted to the phosphate solution in 2 weeks. Interestingly, Activated Carbon, Basolite C300, Basolite A100, and Basolite Z377 reached saturation level around the 7<sup>th</sup> day.

## pH 5 Concentration vs Time

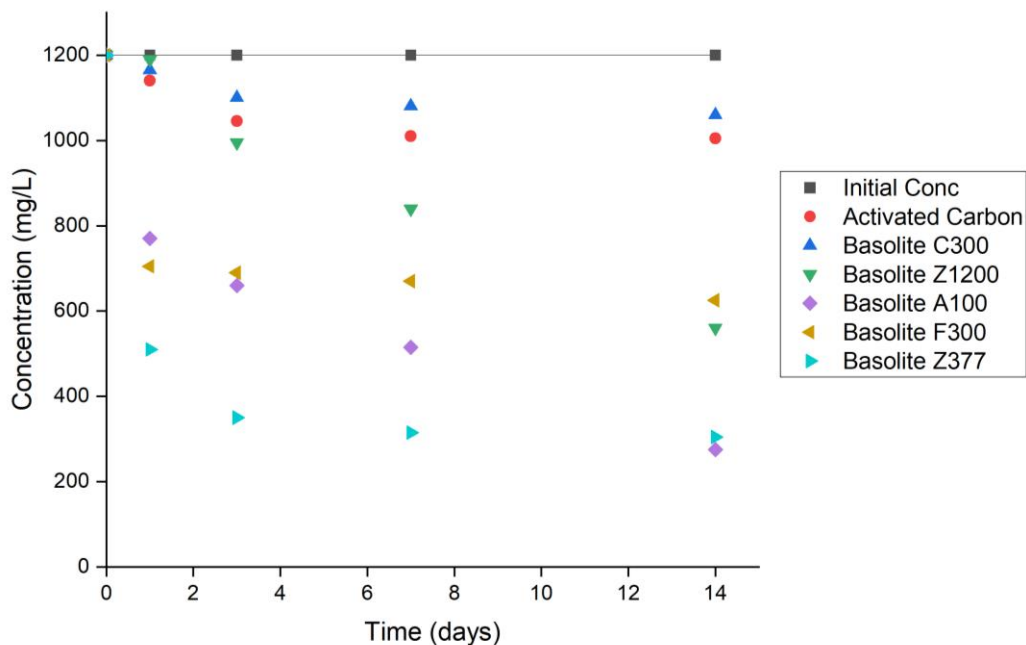


Figure 26, Concentration Vs Time graph of pH 5 after 2 weeks

Similarly, the initial concentration of the solution with pH 7 was measured to be 2.30mg/L.

Table 5 shows the spectrophotometer values of the concentration of the solution at pH 7 after 14 days.

pH 7						
Spectrometer reading	Time Day 0	Day 1	Day 3	Day 7	Day 14	Capacity (mg/g)
Activated Carbon	2.3	2.2	2.18	2.13	2.02	<b>27.95</b>
Basolite C 300	2.3	2.28	2.23	2.09	2.02	<b>37.84</b>
Basolite Z 1200	2.3	2.16	2.06	1.86	1.83	<b>46.86</b>
Basolite A 100	2.3	1.58	0.84	0.74	0.57	<b>172.31</b>
Basolite F 300	2.3	1.29	1.19	0.96	0.93	<b>136.43</b>
Basolite Z 377	2.3	0.69	0.64	0.58	0.52	<b>177.50</b>

Table.5, Spectrophotometer readings of pH 7 after 14 days and the calculated capacity

The capacity values were like pH 5 except for Basolite Z1200 which was lesser than pH 5 meaning that Z1200 performed at pH 5. From Fig. 24, Activated Carbon, Basolite C300, Basolite Z1200, Basolite F300, and Basolite Z377 reached saturation level around the 7<sup>th</sup> day.

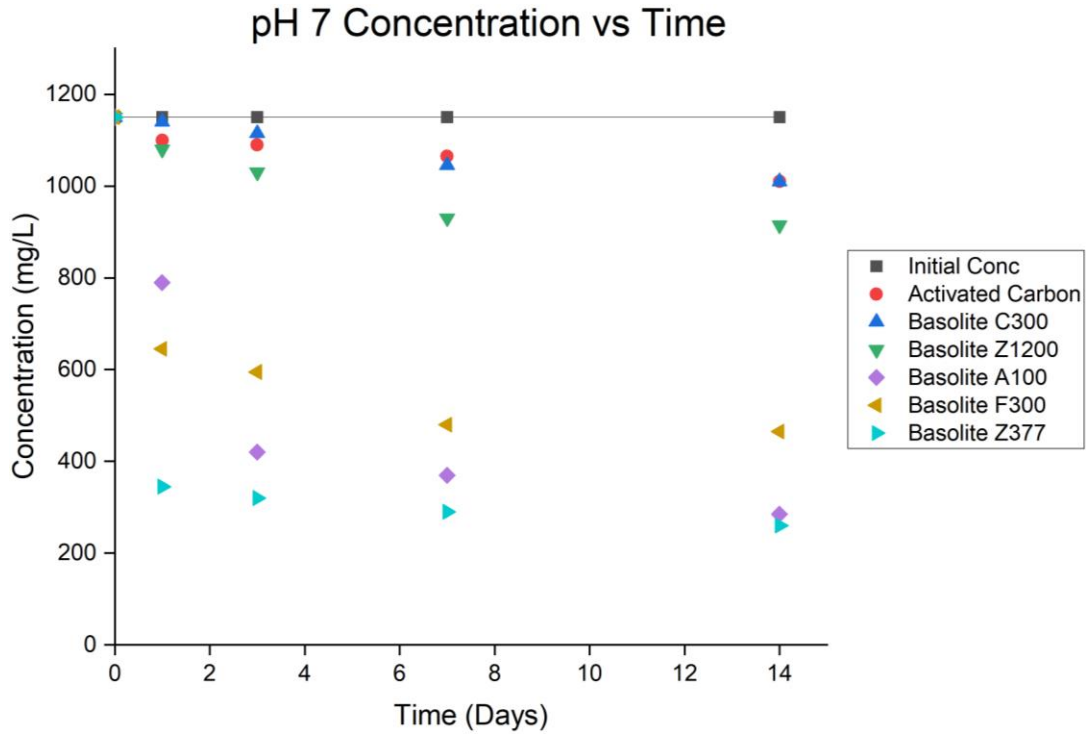


Figure 27, Concentration Vs Time graph of pH 7 after 2 weeks

Likewise, the initial concentration of the solution with pH 9 was measured to be 2.15mg/L.

Table.6 shows the spectrophotometer values of the concentration of the solution at pH 9 after 14 days.

pH 9						
Spectrometer reading	Day 0	Day 1	Day 3	Day 7	Day 14	Capacity (mg/g)
Activated Carbon	2.15	2.12	2.09	1.97	1.91	<b>23.75</b>
Basolite C 300	2.15	2.1	2.08	1.92	1.85	<b>29.83</b>
Basolite Z 1200	2.15	2.08	2.02	1.97	1.77	<b>37.51</b>
Basolite A 100	2.15	0.61	0.53	0.4	0.2	<b>194.03</b>
Basolite F 300	2.15	1.04	0.83	0.73	0.59	<b>154.46</b>
Basolite Z 377	2.15	0.38	0.36	0.33	0.16	<b>198.56</b>

Table.6, Spectrophotometer readings of pH 9 after 14 days and the calculated capacity

From the capacity values, it is noticeable that the adsorbents performed similarly at both pH 7 and pH 9. Here, Activated Carbon, Basolite C300, and Basolite Z1200 have saturated around 7<sup>th</sup> day. In conclusion, most of the adsorbents have reached saturation level at some pHs. Basolite Z377 have performed the best comparing other adsorbents.

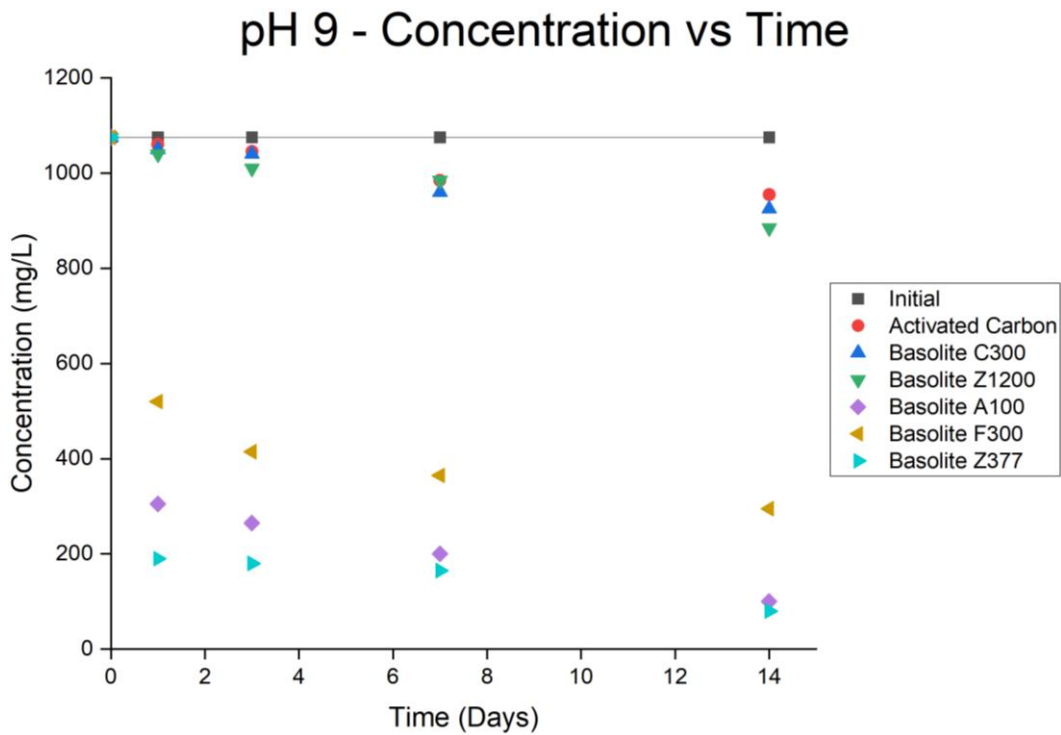


Figure 28, Concentration Vs Time graph of pH 7 after 2 weeks

### 7.2.2. Freundlich Isotherm Results

From the spectrophotometer results log of final concentration and log of capacity at each data point (1day, 3days, 7days, and 14days) and then the graph was plotted. Then linear fitting was done, and the slope and intercept value was taken. The Freundlich isotherm was given as

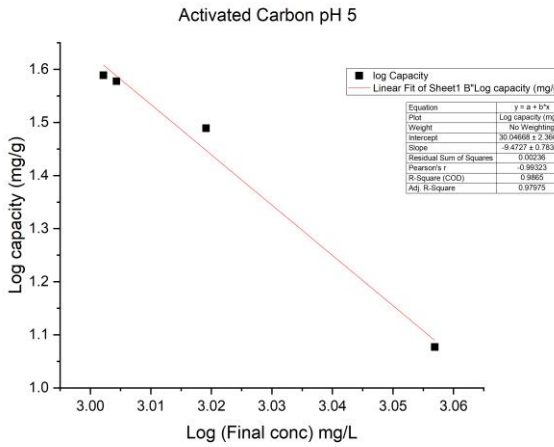
$$q_e = K_F C_e^{1/n}$$

Where  $K_F$  is Freundlich's constant, and  $1/n$  is the exponent of non-linearity.  $C_e$  is the final concentration.  $K_F$  is calculated from the intercept, which is the antilog of intercept value.  $1/n$  is the slope value from the plot. Below is the table of values corresponding to the adsorbents.

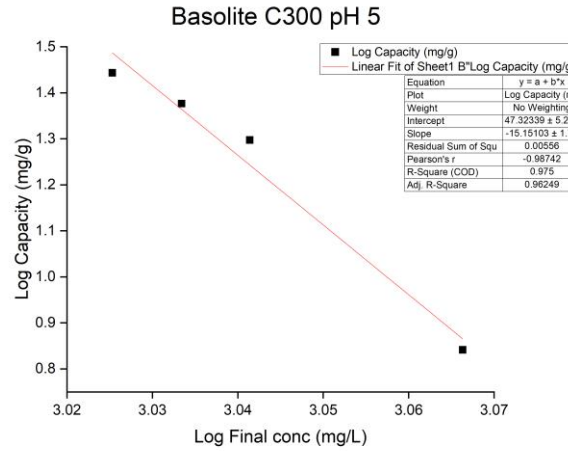
pH 5					
Adsorbent	Intercept	Slope (1/n)	$K_f$	$R^2$	Freundlich Isotherm
Activated Carbon	30.05	-9.4727	1.11E+30	0.98	40.56
Basolite C300	47.32	-15.15103	2.11E+47	0.96	30.68
Basolite Z1200	7.98	-2.10103	9.58E+07	0.96	105.55
Basolite A100	3.99	-0.70108	9874.156	0.91	192.46
Basolite F300	5.51	-1.23541	326572.79	1.00	114.79
Basolite Z377	3.53	-0.51381	3392.42	0.99	179.49

Table 7, Freundlich Isotherm Calculations for pH 5

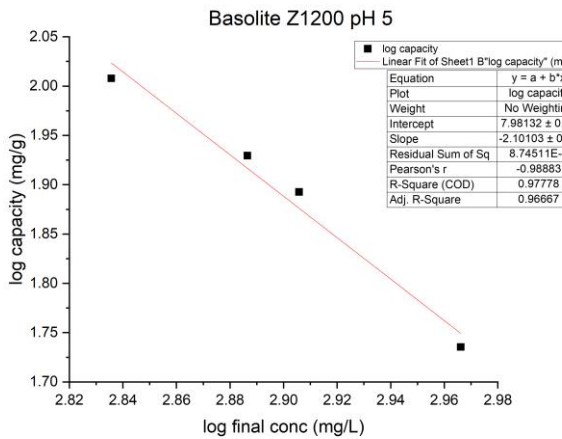
Fig 28 represents the isotherm plots of pH 5. The graph is plotted between log of final conc and log of final capacity. Basolite Z1200 shows nonlinearity while the rest of the adsorbents shows linearity and falls under second order reaction.



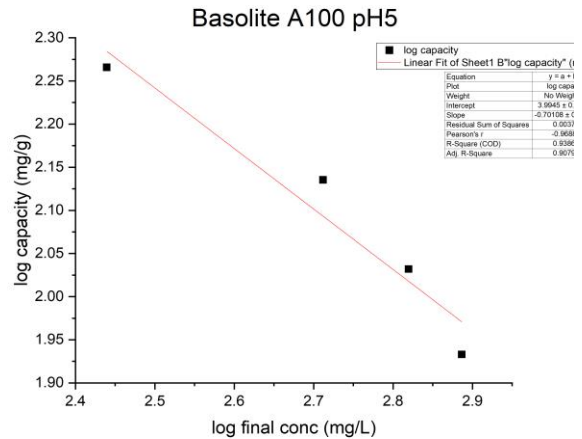
a) pH 5 – Activated Carbon



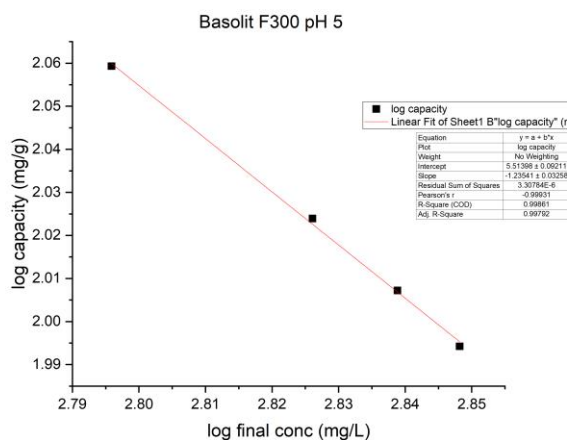
b) pH 5 – Basolite C300



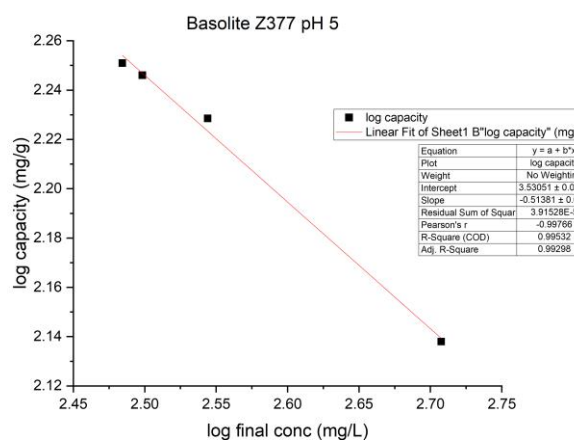
c) pH 5 – Basolite Z1200



d) pH 5 – Basolite A100



e) pH 5 – Basolite F300



f) pH 5 – Basolite Z377

Figure 29, Freundlich Isotherm plot, log final conc vs log capacity.

Table 8 consists of Freundlich isotherm values of pH 7. The Freundlich isotherm values calculated are also closely related to the capacity value. Here Basolite C300 shows nonlinearity.

Adsorbents	intercept	slope (1/n)	$K_f$	$R^2$	Freundlich Isotherm
Activated Carbon	36.65	-11.71	$4.43+36$	0.97	28.93
Basolite C300	62.63	-20.33	$4.25E+62$	0.86	62.63
Basolite Z1200	22.51	-7.03	$3.27E+22$	0.96	48.82
Basolite A100	4.49	-0.90	30831.88	0.94	188.30
Basolite F300	4.59	-0.92	38881.23	0.99	137.08
Basolite Z377	3.10	-0.35	1272.80	0.99	177.85

Table 8, Freundlich Isotherm Calculations for pH 7

Table 9 consists of Freundlich isotherm values of pH 9. The Freundlich isotherm values calculated are also closely related to the capacity value. Here Basolite Z1200 shows nonlinearity.

<b>Adsorbents</b>	<b>intercept</b>	<b>slope (1/n)</b>	<b>K<sub>f</sub></b>	<b>R<sup>2</sup></b>	<b>Freundlich Isotherm</b>
Activated Carbon	58.61	-19.18	4.04E+58	0.93	27.38
Basolite C300	43.23	-14.06	1.70E+43	0.96	33.30
Basolite Z1200	30.01	-9.64	1.01E+30	0.89	40.92
Basolite A100	2.70	-0.20	5.01E+02	0.95	195.88
Basolite F300	3.68	-0.60	4.77E+03	0.97	157.24
Basolite Z377	2.55	-0.13	3.54E+02	0.99	198.73

Table 9, Freundlich Isotherm Calculations for pH 9

### 7.2.3. X-Ray Diffraction

XRD analysis was done samples which were vacuum dried after 14 days. The XRD graph looked like the ‘as bought’ powder before treatment implying that the phosphate adsorption did not alter the crystallinity property of the adsorbent.

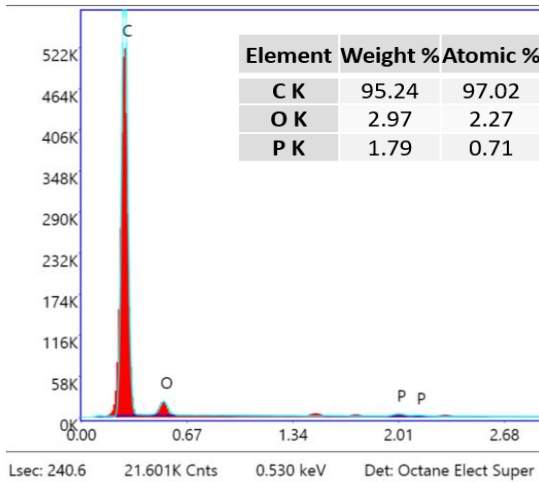
### 7.2.4. SEM

SEM images were taken for the adsorbents after treatment of 14 days. The SEM images of the after-treatment adsorbents are like the images of adsorbents before treatment. It indicates that the phosphate adsorption did not modify the morphology of the adsorbents.

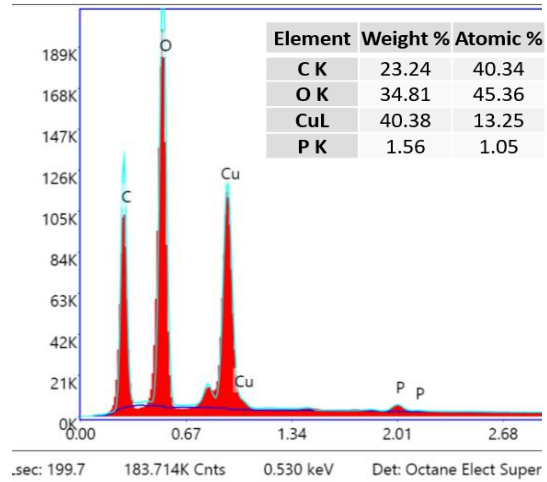
### 7.2.5. EDS

From the graphs, it is obvious that the adsorbent before treatment has no phosphorus when the after-treatment data after 24 hours shows the existence of phosphorus. The images below show

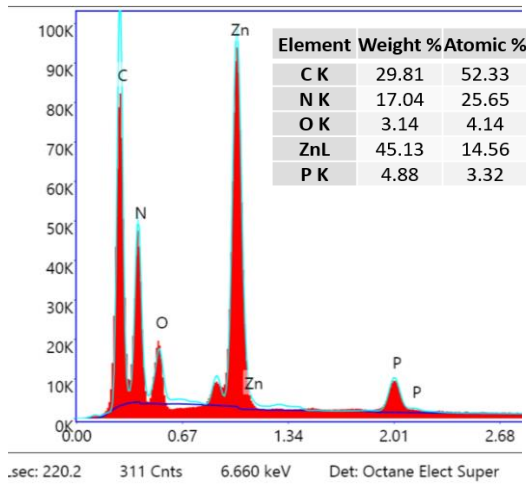
the comparison between before and after treatment of the adsorbents. The phosphorus percentage present after the 14-day experiments are more than the 24 hours experiments.



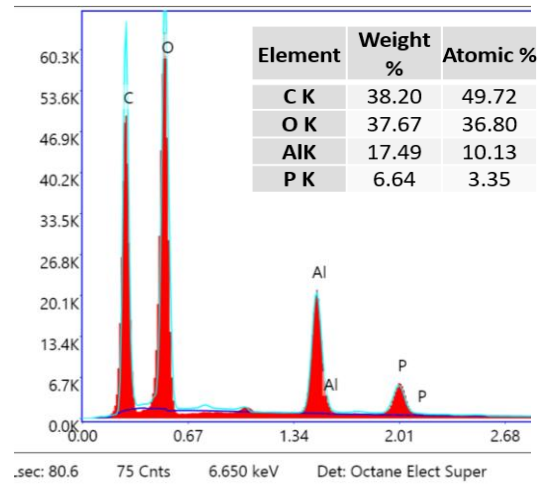
a) pH 5 – Activated Carbon



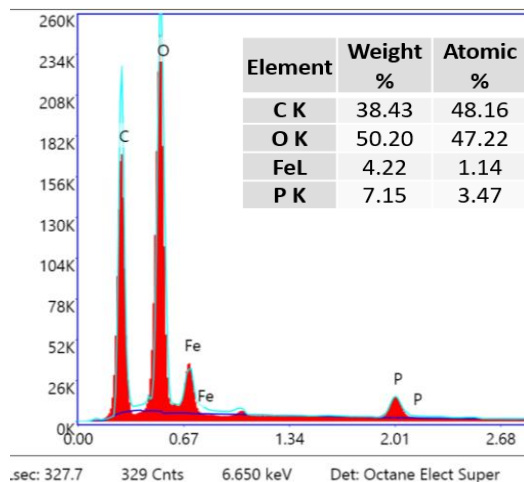
b) pH 5 – Basolite C300



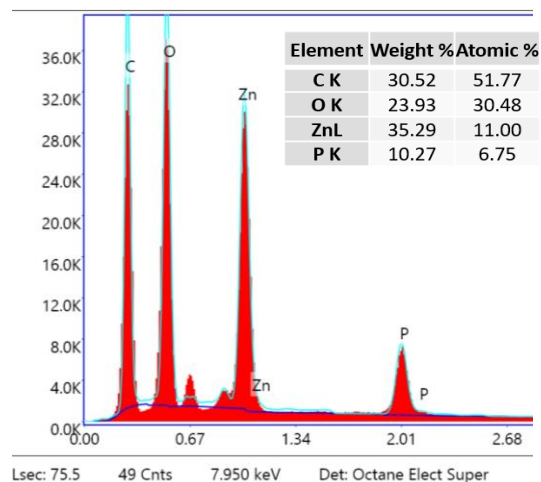
c) pH 5 – Basolite Z1200



d) pH 5 – Basolite A100



e) pH 5 - Basolite F300



f) pH 5 – Basolite Z377

Figure 30, EDAX graph of the adsorbents after adsorption.

### 7.3. FACTORS AFFECTING ADSORPTION

There are various parameters that affect adsorption such as surface area, the nature of adsorbate, the chemical affinity, pore space, particle size, initial concentration, inter-molecular reaction, temperature, and pressure. [29]

One such factor, which is the surface area, was studied compared to the capacity. Below is the table of surface area and the capacity value of pH 5 after 24hours compared.

Adsorbents	Surface Area (m <sup>2</sup> /g)	Capacity (mg/g)	Capacity/Surface Area (mg/m <sup>2</sup> )
Basolite C300	2200	10.97	4.988 X 10 <sup>-3</sup>
Basolite Z1200	1310	19.48	14.87 X 10 <sup>-3</sup>
Basolite A100	1110	96.38	86.82 X 10 <sup>-3</sup>
Basolite F300	1300	82.81	63.70 X 10 <sup>-3</sup>
Basolite Z377	5010	106.47	21.25 X 10 <sup>-3</sup>

Table.10, Capacity vs Surface Area

From the table, Basolite A100 has worked better followed by Basolite F300 and Basolite Z377 than other adsorbents when studied based on the surface area factor. Even though Basolite Z377 has the largest surface area, when compared to the capacity value it is apparent that there are other factors affecting the adsorption as well. Also from the graphs, there was a sudden drop in concentration after just 1 hour in adsorbents such as Basolite F300, Basolite A100, Basolite Z377 then which the concentration has decreased linearly. It is maybe due to the factor of chemical affinity. The larger vacant sites present in the adsorbent to adsorb phosphate might be the reason for the sudden drop after just one hour and then when the pores were getting filled by phosphate ions the drop was linear. [30]

The order of the reaction of pH 7 was observed to be different for the adsorbents. For Basolite C300, first order kinetics was observed while Basolite A100 and Activated Carbon followed second order reaction. Meanwhile, Basolite Z1200, Basolite F300 and Basolite Z377 had pseudo second order kinetics taken place.

#### 7.4. MASS VS CONCENTRATION

To study the absorptivity of the adsorbent, a mass vs concentration study was conducted. Basolite Z377 was chosen for this study. pH 5 solution was used with the initial concentration of 2.30mg/L. The experiment was conducted for one week.

<b>Mass (grams)</b>	<b>Concentration (mg/L)</b>	<b>Capacity (mg/g)</b>
0.1004	980	169.3
0.2000	805	172.5
0.3004	630	173.1
0.4000	460	172.5
0.5004	295	170.9

Table.11, Mass vs Concentration and Capacity

From the above table and the graph, it is noticeable that the concentration is directly proportional to the mass of the adsorbent. Also plotting the graph between the mass and capacity of the adsorbent it is found that the capacity of the adsorbent in various mass got similar values intending that the Basolite Z377 attained saturation in one week and the values are approximately around 170mg/L which also matches with the two week Freundlich isotherm experiment data.

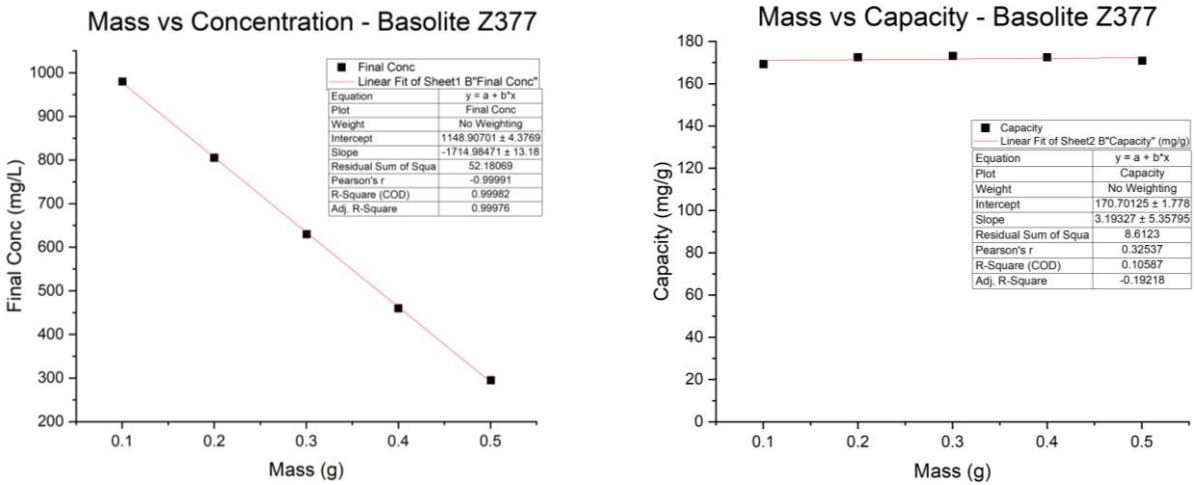


Figure 31, Mass vs Concentration and Mass vs Capacity graph

## 8. CONCLUSION AND FUTURE WORK

Spectrometer Experiments were performed and the kinetics and Freundlich isotherm calculations were done. From the results it is evident that Basolite A100, Basolite F300 and Basolite Z377 have better adsorption abilities when compared with other MOFs and activated carbon. There is also influence of pH in the adsorption as well. Some of the adsorbents show differences in adsorption value based on the pH. Activated Carbon, Basolite C300 and Z1200 have better kinetics results at pH 7 while Activated Carbon and Basolite Z1200 performed better at pH 5 of isotherm experiment. Basolite A100, F300 and Z377 have performed better at pH 9 solution in both kinetics and isotherm experiments. Also, from the XRD and SEM it is noticeable that the phosphate adsorption did not alter the crystallinity property and the adsorbents morphology. From the EDS graphs we can confirm that adsorption has taken place since the EDS gives the surface elemental characterization.

In applications for water treatment, the removal capability of MOFs will be examined in relation to several parameters, including the mass/Volume ratio of adsorbent to the solution, and temperature. Recyclability of MOFs will be determined. Moreover, batch adsorption studies will be conducted to various materials doped MOFs to prove adsorption ability, evaluate the results against commercially available MOFs, assess equilibrium adsorption capacity, and establish adsorption kinetics. The reaction kinetics and mechanism of phosphate decomposition will be examined, and suggestions for integration into the actual application will be given. Further research is needed to investigate the performance and stability of MOFs in real-world applications.

## 9. REFERENCES

- [1] "Phosphate in Surface Water Streams, Lakes, and Ponds," 2020. [Online]. Available: <https://www.knowyourh2o.com/outdoor-4/phosphate-in-surface-water-streams-lakes-ponds>.
- [2] "United States Geological Survey (USGS)," United States Government, 5 June 2018. [Online]. Available: <https://www.usgs.gov/special-topics/water-science-school/science/phosphorus-and-water#overview>. [Accessed 21 February 2023].
- [3] "What is Activated Carbon?," TIGG, 2022. [Online]. Available: <https://tigg.com/resources/activated-carbon-knowledge-base/what-is-activated-carbon/>. [Accessed 03 2023].
- [4] J. C.-M. G. Blanco-Brieva, "Efficient solvent regeneration of Basolite C300 used in the liquid-phase adsorption of dibenzothiophene," *Fuel*, vol. 113, pp. 216-220, 2013.
- [5] B. P., "Zn Based Metal Organic Framework as Adsorbent Material for Mecoprop," *Research Journal of Recent Sciences*, vol. 2, no. 7, pp. 84-86, 2013.
- [6] A. S. Cole Grinnell, "The solid-state synchronous vs. conventional fluorescence spectroscopy and complementary methods to study the interactions of aluminum metal-organic framework Basolite A100 with dimethyl sulfoxide," *Journal of Luminescence*, vol. 210, pp. 485-492, 2019.
- [7] C. G. a. A. Samokhvalov, "Exploring the electronic structure of aluminum metal-organic framework Basolite A100: solid-state synchronous fluorescence spectroscopy reveals new charge excitation/relaxation pathways," *Physical Chemistry Chemical Physics*, vol. 20, no. 42, pp. 26947-26956, 2018.
- [8] B. S. Sylwia Gwardiak, "Benzene adsorption on synthesized and commercial metal-organic frameworks," *Journal of Porous Materials*, vol. 26, p. 775-783, 2018.
- [9] I. Y. Mohammad A Al-Ghouti, "Characterization of diethyl ether adsorption on activated carbon using a novel adsorption refrigerator," *Chemical Engineering Journal*, vol. 162, no. 1, pp. 234-241, 2010.
- [1] "What is a spectrophotometer/Color spectro?," x-rite, [Online]. Available: <https://www.xrite.com/learning-color-education/other-resources/what-is-a-spectrophotometer>. [Accessed 27 march 2023].
- [1] "Instrumentation of a UV-Visible Spectrophotometer," jasco, [Online]. Available: <https://jascoinc.com/learning-center/theory/spectroscopy/uv-vis-spectroscopy/instrumentation/>. [Accessed 23 march 2023].

- [1] "DR1900 Portable Spectrophotometer," HACH, [Online]. Available: <https://www.hach.com/p-dr-1900-portable-spectrophotometer/DR1900-01H#resources>. [Accessed 27 march 2023].
- [1] "Tutorial on Powder X-ray Diffraction for," *ACS Nano*, vol. 13, pp. 7359-7365, 2019.  
3]
- [1] "What is SEM? Scanning Electron Microscopy Explained," ThermoFisher scientific, [Online].  
4] Available: <https://www.thermofisher.com/blog/materials/what-is-sem-scanning-electron-microscopy-explained/>. [Accessed 27 march 2023].
- [1] B. G. & C. Protter, "Energy-Dispersive X-ray Spectroscopy (EDS)," in *MATERIALS CHARACTERIZATION FUNDAMENTALS*, Franklin & Marchall College, 2022, pp. 33-34.  
5]
- [1] M. R. P.S. Sharanyakanth, "Synthesis of metal-organic frameworks (MOFs) and its application in  
6] food packaging: A critical review," *Trends in Food Science & Technology*, vol. 104, pp. 102-116, 2020.
- [1] M. O. Usman and G. Aturagaba, "A review of adsorption techniques for removal of phosphates  
7] from wastewater," *Water Science & Technology*, vol. 86, no. 12, p. 3113–3132, 2022.
- [1] "Characterization of materials: What techniques are used?," ATRIA Innovation, 9 March 2023.  
8] [Online]. Available: <https://www.atriainnovation.com/en/characterization-of-materials-what-techniques-are-used/#:~:text=Materials%20characterization%20is%20the%20process,right%20material%20for%20specific%20applications..> [Accessed 2 April 2023].
- [1] M. P. Hongwei Fan, "MOF-in-COF molecular sieving membrane for selective hydrogen separation,"  
9] *Nature Communications*, vol. 12, pp. 1-10, 2021.
- [2] M. Berger, "Nanowerk," [Online]. Available: <https://www.nanowerk.com/mof-metal-organic-framework.php>. [Accessed 02 april 2023].  
0]
- [2] S. Brandani, "Kinetics of liquid phase batch adsorption experiments," *Adsorption*, vol. 27, p. 353–  
1] 368, 2021.
- [2] V. K.-K. Mahdih Mozaffari Majd, "Adsorption isotherm models: A comprehensive and systematic,"  
2] *Science of the Total Environment*, vol. 812, no. 151334, pp. 1-28, 2022.
- [2] J. APPEL, "FREUNDLICH'S ADSORPTION ISOTHERM," *SURFACE SCIENCE*, vol. 39, pp. 237-244, 1973.  
3]
- [2] S. C. B. Robert J. Umpleby II, "Application of the Freundlich adsorption isotherm in the  
4] characterization of molecularly imprinted polymers," *Analytica Chimica Acta*, vol. 435, pp. 35-42, 2001.

- [2 H.-F. L. X.-R. J. Z.-Y. W. X. L. Y.-Y. Q. Fang-Fang Chen, "Characteristic and model of phosphate adsorption by activated carbon," *Separation and Purification Technology*, vol. 236, no. 116285, pp. 1-12, 2020.
- [2 T. P. Sagar, "Adsorptive Removal of Hazardous Waste Materials using Metal-Organic Frameworks," 6] *International Conference on Multidisciplinary Research & Practice*, vol. 1, no. 8, pp. 469-471.
- [2 E. M. P.-M. Jos´e Elías Conde-Gonz´alez, "Synthesis, performance and mechanism of nanoporous 7] Fe-(1,3,5-tricarboxylic acid) metal-organic framework in the removal of anionic dyes from water," *Environmental Nanotechnology, Monitoring & Management*, vol. 16, no. 100541, pp. 1-9, 2021.
- [2 K. F. C.M. Parish, "Application of STEM Characterization for Investigating Radiation Effects in BCC 8] Fe-Based Alloys," *Journal of Materials Research volume*, vol. 30, p. 1275–1289, 2015.
- [2 Brinkart.com, "Factors Affecting Adsorption," brinkart, [Online]. Available:  
9] [https://www.brinkart.com/article/Factors-Affecting-Adsorption\\_35881/](https://www.brinkart.com/article/Factors-Affecting-Adsorption_35881/). [Accessed 14 May 2023].
- [3 A. B. A. J. LYKLEMA, "Physical and Chemical Adsorption of Ions in the Electrical Double Layer on 0] Hematite," *Journal of Colloid and Interface Science*, vol. 43, no. 2, pp. 437-448, 1973.